PubSub-VFL: Towards Efficient Two-Party Split Learning in Heterogeneous Environments via Publisher/Subscriber Architecture

Yi Liu[1], **Yang Liu**[2,*], **Leqian Zheng**[1], **Jue Hong**[2], **Junjie Shi**[2], **Qingyou Yang**[2], **Ye Wu**[2], **and Cong Wang**[1,*]
[1]Department of Computer Science, City University of Hong Kong
[2]ByteDance Inc.
{yiliu247-c, leqizheng2-c}@my.cityu.edu.hk, congwang@cityu.edu.hk
{liuyang.fromthu, tanzhuo.107, shijunjie.george}@bytedance.com
{yangqingyou, wuye.2020}@bytedance.com

Abstract

With the rapid advancement of the digital economy, data collaboration between organizations has become a well-established business model, driving the growth of various industries. However, privacy concerns make direct data sharing impractical. To address this, Two-Party Split Learning (a.k.a. Vertical Federated Learning (VFL)) has emerged as a promising solution for secure collaborative learning. Despite its advantages, this architecture still suffers from low computational resource utilization and training efficiency. Specifically, its synchronous dependency design increases training latency, while resource and data heterogeneity among participants further hinder efficient computation. To overcome these challenges, we propose PubSub-VFL, a novel VFL paradigm with a Publisher/Subscriber architecture optimized for two-party collaborative learning with high computational efficiency. PubSub-VFL leverages the decoupling capabilities of the Pub/Sub architecture and the data parallelism of the parameter server architecture to design a hierarchical asynchronous mechanism, reducing training latency and improving system efficiency. Additionally, to mitigate the training imbalance caused by resource and data heterogeneity, we formalize an optimization problem based on participants' system profiles, enabling the selection of optimal hyperparameters while preserving privacy. We conduct a theoretical analysis to demonstrate that PubSub-VFL achieves stable convergence and is compatible with security protocols such as differential privacy. Extensive case studies on five benchmark datasets further validate its effectiveness, showing that, compared to state-of-the-art baselines, PubSub-VFL not only accelerates training by $2 \sim 7\times$ without compromising accuracy, but also achieves a computational resource utilization rate of up to 91.07%.

1 Introduction

In the digital economy, data has become a crucial resource driving technological advancements in sectors like autonomous driving [1], healthcare [2], and e-commerce [3]. In this context, enterprises are increasingly collaborating to aggregate diverse data sources to train Machine Learning (ML) models, improving user experience and efficiency [4, 5]. However, centralized data collection poses significant privacy risks and potential breaches [6]. Additionally, regulations like the General Data Protection Regulation (GDPR) [7] impose strict limits on data aggregation and usage, requiring explicit consent and robust safeguards.

[*]Cong Wang and Yang Liu are the corresponding authors.

To address the above privacy concerns, enterprises generally deploy Two-Party Split Learning [8–10] (a.k.a. Vertical Federated Learning (VFL) [11–14]) to collaboratively train ML models without accessing the original data, as shown in Fig. 1. Specifically, in VFL, the data is partitioned vertically, such that each party stores data corresponding to the same sample IDs but with different feature spaces [13, 15, 16]. This allows for a comprehensive analysis through a secure exchange of intermediate results, protecting sensitive data while facilitating joint model training [11, 17]. A notable example is the cooperation between banks and insurance companies aiming to train a model to predict a customer's credit score, a common interest for both entities. Each party holds data on the same individuals but in different feature spaces: banks maintain financial transaction records, while insurance companies retain car accident reports. Due to privacy concerns, regulatory constraints (such as GDPR and HIPAA [18]), and communication network limitations, these features must remain localized within each party. In such scenarios, the VFL approach becomes essential. Therefore, many efforts [19, 2, 20] have been invested in VFL research to further unlock the commercial value of data.

In SL-based VFL[2], each party trains a partial deep network up to a specific layer known as the cut layer (called *bottom model*), which maps raw data features into meaningful vector representations or *embeddings* for prediction tasks. These embeddings are securely transmitted (using methods like differential privacy [21], homomorphic encryption [4], or secure two-party computation [2]) to the *active party*, which holds the labeled data. The active party completes the training using the remaining part of the network (called *top model*) without accessing the raw data of the other parties, thus completing a forward propagation round. Subsequently, gradients are back-propagated from the final layer of the top model to the cut layer. Only the gradients at the cut layer are sent back to the *passive party*, who then continues the backpropagation process locally. This iterative process is repeated until the model converges.

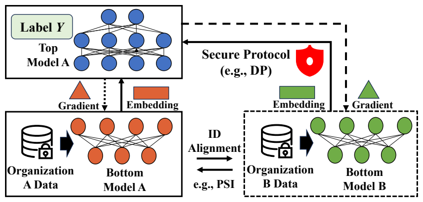

Figure 1: Overview of the split learning (SL)-based VFL framework.

To reduce training costs and resource consumption, researchers and developers have been dedicated to designing efficient VFL architectures to enhance computational resource utilization and improve training efficiency. From a system-level perspective, previous works such as FATE [22] and PaddleFL [23] have focused on achieving efficient data parallelism by employing Parameter Server (PS) [24] architectures, thereby significantly improving computational resource utilization. At the algorithmic level, considerable effort has been devoted to developing effective asynchronous VFL training protocols to optimize computational efficiency [25]. However, these methods still face limitations. Some approaches may not fully address computational bottlenecks, while others might fail to maximize computational efficiency under resource and data heterogeneity conditions. We highlight the reasons behind the above design deficiencies as follows:

- **Neglect of the Decoupling of the System.** Since the VFL with PS setup is still synchronous and tightly coupled, there is a waiting bottleneck between workers on different parties [26], where they either wait for each other or have computational dependencies (see Fig. 6 in Appendix B). Introducing an asynchronous mechanism could potentially improve system decoupling. However, the unique characteristics of the VFL ID alignment [27] present significant challenges in implementing such a mechanism directly (see the detailed analysis in Appendix A).
- **Neglect of the Resource and Data Heterogeneity.** In VFL, computational resource and data feature dimensions often vary significantly among parties, leading to imbalances in computing time [28, 29]. Existing methods typically focus on incrementally improving the computational efficiency of individual parties, overlooking these discrepancies. Thus, the overall computational resources are underutilized due to the lack of a holistic approach to addressing this issue.

To address the limitations of existing approaches, we propose an efficient VFL framework named `PubSub-VFL`, designed to achieve better computational resource utilization and improve training efficiency. `PubSub-VFL` combines the loose coupling advantages of the Publisher/Subscriber (Pub/Sub) architecture with the data parallelism benefits of the PS architecture, enabling flexible asynchronous communication and significantly enhancing system throughput. To further boost computational efficiency and ensure convergence, we design an adaptive semi-asynchronous mechanism within the PS, forming a hierarchical asynchronous mechanism in conjunction with the Pub/Sub asynchrony outside

[2]For the sake of convenience, the term "VFL" is used in the context to refer to the term "SL-based VFL".

the PS. Additionally, to tackle load imbalance issues caused by resource and data heterogeneity, we develop an optimization model that leverages system profile information to determine optimal hyper-parameters, thereby further improving resource utilization. Extensive evaluations on five benchmark datasets demonstrate that `PubSub-VFL` achieves a $2 \sim 7\times$ improvement in computational efficiency over state-of-the-art baselines while maintaining model accuracy.

2 Related Work

Vertical Federated Learning with PS. The integration of PS [24] architectures into (V)FL systems has garnered attention due to its potential to improve scalability and flexibility. Early efforts such as [30] explored using PS architecture to achieve efficient aggregation and distribution of model parameters, simplifying the coordination of multiple participants, but these were primarily focused on horizontal FL settings. More recently, some solutions demonstrated the applicability of PS architectures in VFL contexts, showing improvements in resource utilization and dynamic participant management [26, 22, 23]. Castiglia *et al.* in [31] extended this approach by introducing hierarchical PS architectures, allowing for better load balancing and reduced latency in VFL. However, these solutions still grapple with issues such as decoupling from the unique step in VFL (i.e., ID alignment) to further unlock the potential of PS.

Asynchronous Vertical Federated Learning. Asynchronous training [32–34] methods have gained traction in VFL to address the inefficiencies caused by straggler effects and the need for strict synchronization. Asynchronous VFL (AVFL) enables participants to train and exchange intermediate results independently, significantly improving system throughput and scalability. Recent works, such as those by [34], have demonstrated the efficacy of AVFL in mitigating delays caused by slow participants, thereby enhancing the overall efficiency of the learning process. Nevertheless, asynchronous methods introduce new complexities, including staleness in gradients and potential divergence of models. To tackle these issues, recent research has focused on developing consistency models [35, 36] and adaptive asynchronous strategies [37]. We summarize the comparison between existing methods and `PubSub-VFL` in Table 5 in Appendix A.

3 Problem Formulation

We consider a realistic scenario where two organizations collaboratively train an ML model to perform a prediction task. We then formalize a framework for VFL, with the objective of maximizing the utilization of computing resources between two parties. In VFL, data is vertically partitioned such that each party holds different features for the same set of samples. Specifically, Active Party P_a possesses dataset $D_1 = \{(\mathbf{x}_i^a, y_i)\}_{i=1}^n$, where $\mathbf{x}_i^a \in \mathbb{R}^{d_a}$ represents its feature vectors and $y_i \in \mathbb{R}$ denotes the labels, while Passive Party P_p holds dataset $D_2 = \{\mathbf{x}_i^p\}_{i=1}^n$, with $\mathbf{x}_i^p \in \mathbb{R}^{d_p}$. Note that the features of the two parties are disjoint. The model architecture is split into two parts: the top model and the bottom model, where the bottom models $f_a(\cdot)$ and $f_p(\cdot)$ are held by P_a and P_p, respectively, while the top model $g(\cdot,\cdot)$ is held by P_a which holds the label. Before training begins, P_a and P_p must identify data samples with matching identifiers (such as ID). To preserve the privacy of both parties, Private Set Intersection (PSI) [38] technique is typically employed to securely obtain the "shared" dataset without revealing any private information. During the forward pass, P_p computes an intermediate representation $z_i^p = f_p(\mathbf{x}_i^p)$ (i.e., embeddings) and securely sends it to P_a by using methods like DP protocol, which then computes $z_i^a = f_a(\mathbf{x}_i^a)$ and aggregates these representations using $g(\cdot)$ to produce $\hat{y}_i$, i.e., $\hat{y}_i = g(f_a(\mathbf{x}_i^a), f_p(\mathbf{x}_i^p))$. The loss function $\mathcal{L}(\hat{y}_i, y_i)$ is calculated at P_a. For example, for a classification task, the loss function can be the Cross-Entropy Loss:

$$\mathcal{L}(\hat{y}_i, y_i) = -\frac{1}{n}\sum_{i=1}^{n}\left(y_i \log(\hat{y}_i) + (1-y_i)\log(1-\hat{y}_i)\right). \tag{1}$$

In the backward pass, P_a computes gradients $\nabla_{z_i^a}\mathcal{L}$ and $\nabla_{\theta_1}\mathcal{L}$, sending $\nabla_{z_i^p}\mathcal{L}$ back to P_p, which uses it to compute $\nabla_{\theta_2}\mathcal{L}$. Both parties update their local model parameters using gradient descent:

$$\theta_1 \leftarrow \theta_1 - \eta\nabla_{\theta_1}\mathcal{L}, \theta_2 \leftarrow \theta_2 - \eta\nabla_{\theta_2}\mathcal{L}, \tag{2}$$

where η is the learning rate, and θ_1 and θ_2 are the network parameters of f_1 and f_2, respectively.

To maximize the utilization of computational resources, we need to balance the computational load between the two parties. Let $Cost_A$ denote the computational cost of P_a for processing f_a and

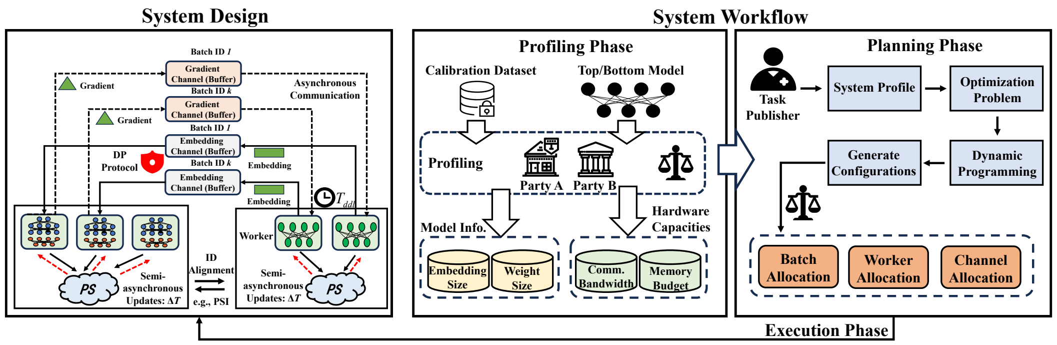

Figure 2: System architecture and workflow of `PubSub-VFL`.

$Cost_P$ denote the computational cost of P_p for processing f_p. We use T_A to denote the total time taken by P_a for one iteration and use T_P to denote the total time taken by P_p for one iteration. The goal is to minimize the maximum time taken by either party, i.e., minimize $\max(T_A, T_P)$. Assuming that the communication overhead is not negligible, we can write:

$$T_A = Cost_A + t_g, T_P = Cost_P + t_e, \tag{3}$$

where t_g is time for sending gradient $\nabla_{\theta_2}\mathcal{L}$ and t_e is time for sending z_i^p. To balance the load, we aim to equalize T_A and T_P: $T_A \approx T_P$. This can be achieved by adjusting the training efficiency of f_a and f_p or dynamically allocating computing resources. For example, if $Cost_A > Cost_P$, we can improve the training efficiency of f_a or increase the training efficiency of f_p to balance the workload. The formal objective is to minimize the maximum time taken by either party while ensuring convergence of the model:

$$\min \max(T_A, T_P), \tag{4}$$

subject to: $\frac{1}{n}\sum_{i=1}^{n} \mathcal{L}(\hat{y}_i, y_i) \leq \kappa$, where κ is a small tolerance for the loss.

Discussion. Optimizing Eq. (4) is a challenging task due to two key factors: 1) **Resource and Data Heterogeneity.** In practice, P_a and P_p often differ significantly in their computing resources and data dimensions. Additionally, P_p's computational overhead in VFL is notably lower than P_a's, as P_p does not need to perform a backward pass of the top model. Therefore, it is essential to balance resource allocation while accounting for the computational complexities of both parties. 2) **Privacy Restrictions.** Due to privacy concerns, it is not feasible to manage and control resource allocation in a centralized manner. This limitation distinguishes the problem from traditional resource scheduling in VFL, requiring more nuanced approaches to ensure privacy while optimizing resource utilization.

4 System and Algorithm Design

4.1 System Design

Key Idea. To address the scarecrow solution's limitations (more details can be found in Appendix A), our key idea is to *decouple the data ID alignment task from the training tasks of workers across different parties.* This approach allows workers to focus solely on local training without the need to ensure data ID alignment beforehand. To implement this, we introduce the *Publisher/Subscriber* (Pub/Sub) [39] architecture, which effectively separates the training process from the data ID matching task, enabling asynchronous operations while maintaining the necessary alignment. By doing so, we can eliminate waiting delays, improve system concurrency, and ensure seamless data ID alignment without burdening the workers with additional coordination tasks. More information about the Pub/Sub can be found in the Appendix B.

To this end, we design the `PubSub-VFL` system to support efficient and scalable VFL. As illustrated in Fig. 2, we introduce two types of communication channels: *embedding channels* and *gradient channels*, responsible for transmitting embeddings and gradients, respectively. To decouple data alignment from model training, we assign a unique batch ID to each training batch. This batch ID is used to label both embedding and gradient channels, enabling precise coordination of intermediate results across parties. Each worker sends its outputs to the appropriate channel based on the batch ID, avoiding synchronization delays. Given a total of n training samples and a batch size B, the system maintains $\lceil n/B \rceil$ embedding and gradient channels. This design ensures consistent data alignment while supporting asynchronous training, thereby improving efficiency. In a more practical scenario, computationally efficient workers may generate excessive embeddings or gradients, leading to channel congestion, which can impede model convergence or even cause training failures. To address this, we propose two mechanisms:

- **Buffer Mechanism:** Each channel buffer can store up to p embeddings and q gradients, with each entry timestamped. When the buffer reaches its capacity, it discards the oldest embedding or gradient based on a First-In-First-Out (FIFO) [40] principle to prevent stale updates from affecting the training process.
- **Waiting Deadline Mechanism:** If a subscribing worker does not receive the embedding or gradient from the publishing worker within a predetermined time T_{ddl}, it discards the current batch and notifies the other party to proceed with the next batch. The system then reassigns the batch to any available pair of workers for retraining, ensuring the continuity of the training process and mitigating delays caused by congestion.

Intra-party Semi-asynchronous Mechanism. Building on the Pub/Sub architecture, we achieve inter-party asynchronous communication, effectively eliminating worker-side waiting delays. To further improve computational efficiency within each party (i.e., between the PS and its workers), we extend this design with an intra-party asynchronous mechanism. However, this hierarchical asynchrony can hinder model convergence if not properly controlled. To mitigate this, we propose a dynamic semi-asynchronous mechanism that adaptively regulates the synchronization interval based on training feedback. Specifically, the synchronization interval ΔT_t decreases as the model approaches the target accuracy, striking a balance between computation speed and convergence stability. The interval ΔT_t is defined as:

$$\Delta T_t = \left\lceil \frac{\Delta T_0}{2} \cdot \tanh\left(\frac{2 \cdot t}{\Delta T_0} - 2\right) + \frac{\Delta T_0}{2} \right\rceil, \tag{5}$$

where ΔT_0 is the initial asynchronous interval, t is the current training epoch, and $\tanh(\cdot)$ is the hyperbolic tangent function. Initially, when the model is far from the target accuracy, ΔT_t is small, allowing the model to achieve stable learning. As the accuracy increases, the interval increases and the synchronization frequency is reduced to fine-tune the model and ensure faster convergence.

Differential Privacy Protocol. To prevent the embedded information sent by P_p from being inferred by attackers (such as labels or features), specific perturbations must be added to the embeddings. To balance privacy and utility effectively, we adopt Gaussian Differential Privacy (GDP) (see Appdenix C for more details) as outlined in [21, 33] to safeguard the embedding information. In addition, we prove in Appendix D that `PubSub-VFL` integrated GDP protocol can still converge stably.

4.2 System Profiling

Key Idea. `PubSub-VFL` effectively integrates Pub/Sub and PS architectures to harness the computational capabilities of participating parties, substantially improving training efficiency. Nevertheless, the system remains susceptible to latency caused by resource and data heterogeneity. A key challenge lies in optimizing resource allocation collaboratively without violating privacy constraints. To address this, we propose a privacy-preserving parameter optimization strategy that determines optimal configurations, e.g., the number of workers, batch size, and core allocation, based on each party's system profile, including model characteristics and hardware capabilities. By adapting these parameters to individual constraints, the system achieves balanced workload distribution, reduced latency, and improved overall efficiency, all while preserving data privacy.

To achieve this goal, we first model the computation and communication delays of both the active and passive parties in the designed `PubSub-VFL` system. For the P_a, we denote the number of workers as $w_a \in [P, Q]$, batch size as B, and total computing cores as C_a. For the P_p, the number of workers is $w_p \in [M, N]$, batch size as B, and total computing cores as C_p. Let $\{c_{a,i}\}_{i=1}^{w_a}$ (where $\sum_{i=1}^{w_a} c_{a,i} \leq C_a$, be the CPU cores allocated to each of the w_a and $\{c_{p,j}\}_{j=1}^{w_p}$ (where $\sum_{j=1}^{w_p} c_{p,j} \leq C_p$) be the CPU cores allocated to each of the w_p. Therefore, the computation delay of the forward pass of both parties can be formally defined as follows:

$$T_f^{(a)}(B) = \frac{\lambda_a B^{\gamma_a}}{\sum_{j=1}^{w_a} c_{a,j}}, T_f^{(p)}(B) = \frac{\lambda_p B^{\gamma_p}}{\sum_{i=1}^{w_p} c_{p,i}}, \tag{6}$$

where $T_f^{(a)}(B)$ is the time for forward pass of the P_a on a batch of size B, $T_f^{(p)}(B)$ is the time for forward pass of the P_p on a batch of size B, γ_a, λ_a, γ_p, and λ_p are the proportionality constants. For simplicity, if all w_p workers are assigned equally, it might become $T_f^{(a)}(B) = \frac{\lambda_a B^{\gamma_a} w_a}{C_a}$ and $T_f^{(p)}(B) = \frac{\lambda_p B^{\gamma_p} w_p}{C_p}$. Similarly, let β_a and β_p be the constant for the backward pass. Thus, we have:

$$T_b^{(a)}(B) = \frac{\varphi_a B^{\beta_a} w_a}{C_a}, T_b^{(p)}(B) = \frac{\varphi_p B^{\beta_p} w_p}{C_p}. \tag{7}$$

We give the forward and backward propagation time of the top model part of P_a as follows:

$$T_{top}^{(a)}(B) = \frac{\lambda_a^{'} B^{\gamma_a^{'}} w_a}{C_a} + \frac{\varphi_a^{'} B^{\beta_a^{'}} w_a}{C_a}. \tag{8}$$

Next, we consider the communication delay within the system pipeline. Let E denote the size of the embedding sent by the P_p and G the size of the gradient sent by the P_a. Each iteration involves two primary communications: P_p sends the embedding to P_a, and P_a sends the gradient back to P_p. Therefore, the total communication delay for each iteration can be expressed as:

$$T_{emb} = \frac{E}{B_b}, T_{grad} = \frac{G}{B_b}. \tag{9}$$

where B_b denotes the bandwidth capacities of the system. Since the semi-asynchronous aggregation within the PS is performed internally within each participant, the communication delays from this step can be ignored, as they are generally fixed constants.

Remark on Pipelining/Asynchronous Pub/Sub. With a Pub/Sub architecture, one can sometimes overlap the next batch's forward pass at the P_p with the P_a's backward pass from the previous batch. In a fully pipelined system with enough buffering, the overall iteration time can be lower than the naive sum above. Nonetheless, many system analyses still approximate iteration time by a "critical path" sum or a maximum of partial sums [41, 42]. For simplicity, we continue with the additive formula here, but in practice, pipelining would reduce that total somewhat.

4.3 System Planning Phase

Optimization Problem Formulation. Due to privacy constraints and restricted network access, participants cannot collaboratively execute fine-grained pipeline operations. To overcome this limitation, we estimate the computation and communication times in the Pub/Sub setting using observations from a synchronous baseline, as illustrated in Fig. 2. These estimations enable the construction of an optimization model to determine the optimal initialization hyperparameters, specifically, the number of workers and batch size. This model aims to balance computation and communication costs while maintaining system efficiency under privacy and network constraints. Based on Eq. (4), the formal expressions for T_A and T_P can be rewritten as:

$$T_A = T_f^{(a)} + T_b^{(a)} + T_{top}^{(a)} + T_{grad}, T_P = T_f^{(p)} + T_b^{(p)} + T_{emb}. \tag{10}$$

Then, we rewrite Eq. (4) as follows:

$$\min \max(T_f^{(a)} + T_b^{(a)} + T_{top}^{(a)} + T_{grad}, T_f^{(p)} + T_b^{(p)} + T_{emb}). \tag{11}$$

In Eq. (11), we want to choose the optimal hyperparameters, i.e., $w_a \in \{P, P+1, \ldots, Q\}$, $w_p \in \{M, M+1, \ldots, N\}$, an integral (or real) batch size $1 \le B \le B_{max}$ (bounded above by some feasible maximum, i.e., memory constraints), to optimize the goal. We assume that each party has its own memory constraint per worker. Thus, we follow [41] to specify the memory usage functions as

$$M_A(B) = M_{A0} + \rho_A B^{\chi}, M_P(B) = M_{P0} + \rho_P B^{\chi}, \tag{12}$$

where M_{A0} and M_{P0} are the base memory consumptions at the active and passive parties respectively, and ρ_A, ρ_P (with exponent χ) capture the extra memory needed per worker as a function of the minibatch size B. If the maximum available memory per worker at the P_a is $\bar{M}_A$ and at the P_p is $\bar{M}_P$, then the memory constraints become $B \leq \left(\frac{\bar{M}_A - M_{A0}}{\gamma_A}\right)^{1/\chi}, B \leq \left(\frac{\bar{M}_P - M_{P0}}{\gamma_P}\right)^{1/\chi}$. Thus, we define the overall feasible maximum batch size due to memory as

$$B_{\max} = \min\left\{\left(\frac{\bar{M}_A - M_{A0}}{\rho_A}\right)^{1/\chi}, \left(\frac{\bar{M}_P - M_{P0}}{\rho_P}\right)^{1/\chi}\right\}. \tag{13}$$

We assume that the candidate minibatch sizes are taken from a discrete set, i.e., $\mathcal{B} = \{B_1, B_2, \ldots, B_R\}$, but only those values that satisfy $B \leq B_{\max}$ are feasible. Since both parties must finish their computations before proceeding to the next iteration, the overall per-iteration delay is the maximum of the two computation delays plus the communication delay:

$$\min \mathcal{O}(w_A, w_P, B) = \min_{w_a, w_p, B \leq B_{\max}} \left\{\max\left(T_f^{(a)} + T_b^{(a)} + T_{top}^{(a)}, T_f^{(p)} + T_b^{(p)}\right) + \frac{E+G}{B_b}\right\}. \tag{14}$$

Dynamic Programming Algorithm Design. Because the decision space (over w_a, w_p, and B) is discrete, we now describe a dynamic programming approach to search for the optimal configuration. We define a dynamic programming state by the triplet (i, j, r), where, i indexes the candidate active worker count: $w_a = M + i - 1$ for $i = 1, 2, \ldots, (N - M + 1)$, j indexes the candidate passive worker count: $w_p = P + j - 1$ for $j = 1, 2, \ldots, (Q - P + 1)$, and r indexes the candidate minibatch size: $B = B_r$ for $r = 1, 2, \ldots, R$, with the additional constraint $B_r \leq B_{\max}$. The cost associated with state (i, j, r) is defined as

$$\begin{aligned}\mathrm{Cost}(i, j, r) = \max\Bigg\{&\frac{(\lambda_a B_r^{\gamma_a} + \lambda_a' B_r^{\gamma_a'} + \varphi_a B_r^{\beta_a} + \varphi_a' B_r^{\beta_a'})(M + i - 1)}{C_a}, \\ &\frac{(\lambda_p B_r^{\gamma_p} + \varphi_a B_r^{\beta_p})(P + j - 1)}{C_p}\Bigg\}.\end{aligned} \tag{15}$$

The objective is to find the state (i^*, j^*, r^*) that minimizes this cost. The above dynamic programming solution (Algo. 2) and the pseudo code of `PubSub-VFL` (Algo. 1) can be found in the Appendix E.

5 Experiment

5.1 Experiment Setup

To evaluate the performance of our `PubSub-VFL` system, we conduct extensive experiments on five datasets. All experiments are developed using Python 3.9 and PyTorch 1.12 and evaluated on a server with an INTEL(R) XEON(R) GOLD 6530 (64-core CPU).

Datasets. We evaluate `PubSub-VFL` on four public benchmark datasets (see Table 6 in Appendix F) spanning both regression and classification tasks, along with a large-scale synthetic dataset. For regression, we use the Energy [43] (19,735 samples, 27 features) and Blog [44] (60,021 samples, 280 features) datasets. For classification, we adopt the Bank [45] (40,787 samples, 48 features) and Credit [46] (30,000 samples, 23 features) datasets. To assess scalability, we generate a synthetic dataset with 1 million samples and 500 features using Scikit-learn [47]. Each dataset is split into 70% training and 30% testing, with training data approximately evenly distributed between two parties. To simulate feature heterogeneity, we vary the number of features assigned to each party.

Table 1: Accuracy comparison results.

Dataset	Metric	VFL	VFL-PS	AVFL	AVFL-PS	Ours
Energy	RMSE	84.58	84.44	85.41	85.39	85.64
Blog	RMSE	23.20	23.12	23.38	23.45	**22.34**
Bank	AUC	94.54	94.13	94.12	94.16	**96.54**
Credit	AUC	81.90	81.34	80.83	80.34	**82.34**
Synthetic	AUC	91.27	91.31	90.97	91.21	**92.87**

Models. For the top model, we use a Multi-Layer Perceptron (MLP) with two layers. For the bottom model, we use two models of different sizes, namely a ten-layer MLP and a ResNet [48], which can verify the performance of `PubSubVFL` under different model sizes.

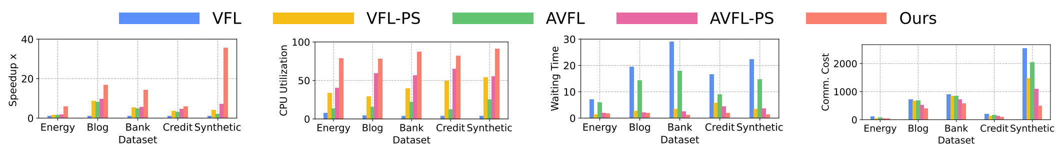

(a) Running Time (b) CPU Utilization (c) Waiting Time (d) Comm. Cost

Figure 3: Comparison with existing baselines in computation and communication efficiency.

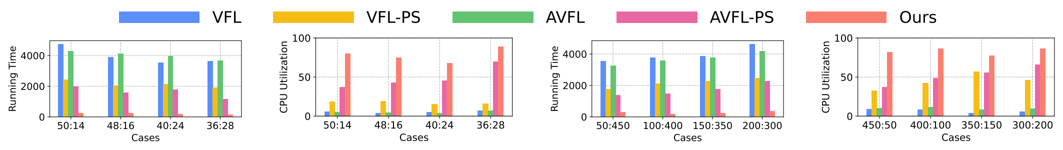

(a) Running Time (b) CPU Utilization (c) Running Time (d) CPU Utilization

Figure 4: Comparison with existing baselines on computation efficiency in resource and data heterogeneous scenarios.

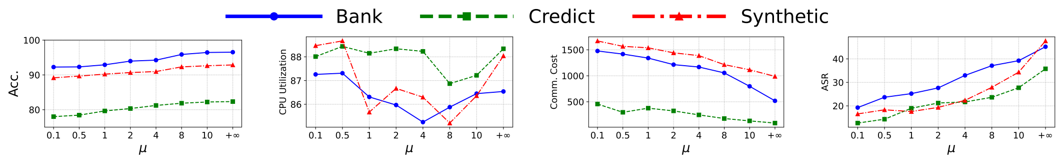

(a) Accuracy (b) CPU Utilization (c) Comm. Cost (d) ASR

Figure 5: The impact of privacy budget on the performance, efficiency, and security of `PubSub-VFL`.

Table 2: Effect of the number of workers.

# of Workers	4	5	**8***	10	20	30	50
Acc.(%)	92.13	92.05	**92.06**	92.28	92.00	92.36	92.21
Time (s)	712.78	805.90	**668.11**	885.01	1420.32	1067.57	1661.74
CPU (%)	67.52	63.30	**88.04**	76.18	42.77	40.78	45.12
Waiting (s)	1.4686	1.9273	**1.5288**	3.461	8.088	9.687	19.843
Comm. (MB)	878.91	1098.63	**888.77**	1318.36	1867.68	1538.09	2197.27

Table 3: Effect of the different batch size.

Batch Size	16	32	64	128	**256**	512	1024
Acc.(%)	91.70	92.06	91.75	92.63	**92.67**	92.36	92.21
Time (s)	987.64	668.11	344.76	124.01	**92.54**	578.69	865.74
CPU (%)	48.64	88.04	90.12	89.97	**91.07**	84.47	52.67
Waiting (s)	1.087	1.5288	1.688	1.263	**1.1389**	1.324	1.789
Comm. (MB)	1298.32	888.77	329.59	439.45	**439.45**	736.89	1070.36

Parameters. For a series of constants, we set $\Delta T_0 = 5$, $T_{ddl} = 10s$, $p = 5$, $q = 5$. For the constants in the optimization model, we determined them through empirical experiments (see the Appendix H for details). In addition, we set the learning rate to 0.001, the number of workers to $w_a/w_p \in [2, 50]$, the batch size $B \in \{16, 32, 64, 128, 256, 512, 1024\}$, and $C_a + C_p = 64$.

Baselines. In this paper, we adopt the following baselines: 1) *Pure VFL:* This is a classic VFL architecture that does not involve the PS architecture or asynchronous mechanisms. 2)*VFL with PS:* This is the most widely adopted VFL architecture in the industry, implemented in mature frameworks such as FATE [22] and PaddleFL [23]. By leveraging the PS architecture, it enhances computational resource utilization and efficiency, enabling more effective parallel processing. 3) *Asynchronous VFL:* Building on traditional VFL, developers can integrate asynchronous mechanisms [32, 34] to implement Asynchronous VFL (AVFL), enhancing system efficiency by reducing idle time and improving parallelism. 4) *Asynchronous VFL with PS:* Building on AVFL, developers can integrate the PS mechanism [26] to further enhance VFL efficiency. Notably, the asynchronous implementation in this architecture is achieved through inter-party communication between parties.

Evaluation Metrics. For the four public benchmark datasets, we evaluate classification tasks using the Area Under the ROC Curve (AUC) and regression tasks using the Root Mean Square Error (RMSE). For the synthetic dataset, we use AUC as the evaluation metric for classification tasks. To fairly assess computational resource utilization, we measure running time, CPU utilization, and waiting time/epoch. Additionally, we record communication cost to compare the communication efficiency of different methods. Results of additional experiments can be found in Appendix H.

5.2 Numerical Results

System Performance. We evaluate the performance of PubSub-VFL and baseline methods on five datasets across classification and regression tasks. To ensure a balanced allocation of resources and data, we evenly distribute CPU cores and feature sizes between the two parties. Additionally, to assess the impact of different bottom model architectures, we employ both MLP and ResNet models. We report the best performance of each method under optimal hyperparameter configurations in Table 1 (small size model) and Table 7 (large size model). The experimental results demonstrate that PubSub-VFL achieves accuracy comparable to or even surpassing baseline methods on the Bank, Credit, and Synthetic datasets. This confirms that integrating the Pub/Sub architecture and semi-asynchronous mechanism does not compromise system performance or convergence.

Comp. & Comm. Costs. We evaluate the computational and communication efficiency of PubSub-VFL against baseline methods. Using our strategy, we set the hyperparameters to $B = 256$, $w_a = 8$, and $w_p = 10$. For computational efficiency, we measure total running time, CPU utilization, and per-epoch waiting time required to reach a target accuracy of 91%. Communication efficiency is assessed via the total communication cost. Experiments on the synthetic dataset show that PubSub-VFL significantly outperforms all baselines in both computation and resource utilization. As shown in Fig. 3, PubSub-VFL achieves a $7\times$ reduction in running time and 35% higher CPU utilization compared to the best-performing baseline, AVFL-PS. These gains stem from reduced worker idle time and improved parallelism. Moreover, the hierarchical asynchronous mechanism enhances convergence efficiency, leading to lower communication cost than other methods.

Resource and Data Heterogeneity Scenarios. We evaluate the computational efficiency of PubSub-VFL and the baseline methods under varying resource allocation and feature size distribution scenarios. For the resource heterogeneous scenario, we set different CPU core ratios between P_a and P_p: 50:14, 48:16, 40:24, and 36:28 (where the first value represents P_a's CPU cores). For the data heterogeneous scenario, we set different feature size ratios: 50:450, 100:400, 150:350, and 200:300. In each scenario, we apply our optimization method to determine the best hyperparameters and configure them for PubSub-VFL. The experimental results, shown in Fig. 4, reveal that in the resource heterogeneous scenario, imbalanced computational efficiency between parties significantly increases waiting time and decreases CPU utilization in baseline methods. Specifically, the CPU utilization of PubSub-VFL is still as high as 87.42% when the CPU core ratio is 50:14, while that of AVFL-PS is only 42.12%. This happens because resource disparities exacerbate computational imbalances, further extending training latency. In contrast, PubSub-VFL effectively balances computational efficiency, reducing running time and maintaining high CPU utilization. In the data heterogeneity scenario, we observe similar trends. Additionally, we find that reducing the data dimension processed by P_a can further decrease running time (as shown in Fig. 4 (c)–(d)). This is because it helps balance the computational load between both parties, aligning with our optimization model design approach.

Security Performance Evaluation. We evaluate it from two dimensions: system performance and defense against embedded inversion attacks [49]. We follow the above hyperparameter configuration to configure PubSub-VFL. For the privacy parameter, we set $\mu \in \{0.1, 0.5, 1, 2, 4, 8, 10, +\infty\}$.

System Performance. We evaluate the impact of μ on PubSub-VFL by recording its accuracy, CPU utilization, and communication cost on the Bank, Credit, and Synthetic datasets. The results, presented in Fig. 5, demonstrate that introducing the DP protocol has minimal effect on accuracy and CPU utilization, indicating that PubSub-VFL maintains its computational efficiency even with privacy protection. However, we observe a notable increase in communication cost due to the added DP noise, which leads to a slower convergence. Nevertheless, the results confirm that PubSub-VFL seamlessly integrates with security protocols while maintaining strong performance.

Defend Against Embedding Inversion Attacks (EIA). Similarly, we record the performance results (i.e., Attack Success Rate (ASR)) of PubSub-VFL against EIA (we adopt it in [49]) on these datasets (more details can be found in the Appendix G). The results are shown in Fig. 5, showing that the introduction of the DP protocol can help PubSub-VFL defend against EIA well.

Parameter Sensitivity Evaluation. We evaluate the impact of different numbers of workers and batch sizes on the performance of PubSub-VFL under the same setting. Specifically, we set $w_a = w_p \in \{4, 5, 8, 10, 20, 30, 50\}$ and $B \in \{16, 32, 64, 128, 256, 512, 1024\}$.

Table 4: Comparison of Different Methods on Various Datasets

Method	**Energy**	**Blog**	**Bank**	**Credit**	**Synthetic**
All (`PubSub-VFL`)	83.94	22.14	96.97	86.07	94.17
w/o T_{all}	84.35	23.17	95.26	85.74	92.86
w/o Dynamic Programming	84.07	22.16	96.33	85.79	93.82
w/o ΔT	85.68	24.11	95.01	84.45	92.07
w/o PubSub	83.98	22.66	95.17	85.93	93.52
w/o T_{all} and Δ	85.81	24.24	94.32	82.69	91.73
VFL	84.24	23.18	94.97	83.42	92.74
VFL-PS	86.14	23.07	94.74	85.44	92.67
AVFL	83.91	22.97	95.02	84.23	91.54
AVFL-PS	84.29	23.15	95.06	82.27	92.21

Effect of the Numer of Workers. We conduct experiments on the Synthetic dataset with $B = 32$, and the experimental results are shown in Table 2. The results show that simply increasing the parallel factor (i.e., w) does not always improve computational efficiency. For example, we find that when $w = 8$, its computation and communication efficiency is the highest. This is because a large parallel factor will lead to slower convergence.

Effect of the Batch Size. Similarly, we conduct experimens on the Synthetic dataset with $w_a = w_p = 8$. Table 3 records the impact of different B on the performance of `PubSub-VFL`. We find that blindly increasing B cannot always improve the computational efficiency of `PubSub-VFL`. For example, we find that when $B = 256$, its computation and communication efficiency is the highest. This is because too large a batch size will also lead to slower convergence. The above results verify that we need a suitable method to find the optimal hyperparameters in the VFL task.

Ablation Studies. We conduct comprehensive ablation studies following the above experimental setup, including the same model architectures, number of clients, and heterogeneous resource settings. Experiments are performed on the Energy, Blog, Bank, Credit, and Synthetic datasets to evaluate the individual contributions of `PubSub-VFL`'s key components. Specifically, to assess the impact of the waiting deadline mechanism, we set the deadline to $T_{all} = 0s$, effectively disabling the mechanism. To evaluate the dynamic programming algorithm, we adopt a fixed worker allocation (i.e., equal numbers of workers on both party sides), removing the adaptive scheduling it enables. For the intra-party semi-asynchronous mechanism, we remove this component while retaining the PS architecture to isolate its effect. Finally, to study the role of the PubSub architecture, we replace it with the AVFL-PS architecture while keeping all other components unchanged. These ablation experiments allow us to disentangle the influence of each design choice on overall system performance. The experimental results are shown in the Table 4. The Waiting Deadline and Intra-party Semi-asynchronous Mechanisms are pivotal to PubSub-VFL's performance, effectively balancing synchronization and asynchrony to mitigate gradient staleness and ensure timely updates. Their removal incurs significant degradation, e.g., up to 2.10% AUC drop on Synthetic and 1.71% on Bank—highlighting their role in stable convergence. The PubSub architecture and dynamic programming contribute more modestly to performance but enhance robustness by alleviating resource heterogeneity and coordination overhead, improving stability under coupled training dynamics.

6 Conclusion

The paper addressed the problem of underutilization of computational resources in VFL by proposing a new framework named `PubSub-VFL`. Specifically, `PubSub-VFL` enhanced computational efficiency by leveraging a Pub/Sub architecture with hierarchical asynchronous mechanism. Furthermore, we theoretically prove the convergence of `PubSub-VFL`. It reduces training latency, improves resource utilization, and maintains strong convergence and privacy guarantees, achieving up to $2 \sim 7\times$ faster training and $\approx 35\%$ better resource efficiency than state-of-the-art baselines.

Limitations. One limitation of `PubSub-VFL` is that it only supports two-party learning and has not yet been able to support multi-party learning. In future exploration work, we will seek ways to support efficient multi-party learning.

Acknowledgements

We thank all anonymous reviewers for their constructive comments. This work was supported in part by the Hong Kong Research Grants Council under Grants CityU 11218322, 11219524, R6021-20F, R1012-21, RFS21221S04, C2004-21G, C1029-22G, C6015-23G, and N_CityU139/21 and in part by the Innovation and Technology Commission (ITC) under the Joint Mainland-Hong Kong Funding Scheme (MHKJFS) under Grant MHP/135/23. This work was also supported by the InnoHK initiative, The Government of the HKSAR, and the Laboratory for AI-Powered Financial Technologies (AIFT).

References

[1] T. Zheng, A. Li, Z. Chen, H. Wang, and J. Luo, "Autofed: Heterogeneity-aware federated multimodal learning for robust autonomous driving," in *Proc. of MobiCom*, 2023.

[2] J. Ogier du Terrail, S.-S. Ayed, E. Cyffers, F. Grimberg, C. He, R. Loeb, P. Mangold, T. Marchand, O. Marfoq, E. Mushtaq, *et al.*, "Flamby: Datasets and benchmarks for cross-silo federated learning in realistic healthcare settings," in *Proc. of NeurIPS*, 2022.

[3] R. Li, Y. Shu, Y. Cao, Y. Luo, Q. Zuo, X. Wu, J. Yu, and W. Zhang, "Federated cross-view e-commerce recommendation based on feature rescaling," *Scientific Reports*, vol. 14, no. 1, pp. 1–19, 2024.

[4] C. Zhang, S. Li, J. Xia, W. Wang, F. Yan, and Y. Liu, "{BatchCrypt}: Efficient homomorphic encryption for {Cross-Silo} federated learning," in *Proc. of USENIX ATC*, 2020.

[5] Y. Li, Y. Sun, Z. Cui, P. Shen, and S. Shan, "Instance-consistent fair face recognition," *IEEE Transactions on Pattern Analysis and Machine Intelligence*, 2025.

[6] K. Liu, S. Hu, S. Z. Wu, and V. Smith, "On privacy and personalization in cross-silo federated learning," in *Proc. of NeurIPS*, 2022.

[7] P. Voigt and A. Von dem Bussche, "The eu general data protection regulation (gdpr)," *A Practical Guide, 1st Ed., Cham: Springer International Publishing*, vol. 10, no. 3152676, pp. 10–5555, 2017.

[8] N. Chandran, D. Gupta, A. Rastogi, R. Sharma, and S. Tripathi, "Ezpc: Programmable and efficient secure two-party computation for machine learning," in *Proc. of EuroS&P*, 2019.

[9] N. Agrawal, A. Shahin Shamsabadi, M. J. Kusner, and A. Gascón, "Quotient: Two-party secure neural network training and prediction," in *Proc. of CCS*, 2019.

[10] M. G. Poirot, P. Vepakomma, K. Chang, J. Kalpathy-Cramer, R. Gupta, and R. Raskar, "Split learning for collaborative deep learning in healthcare," *arXiv preprint arXiv:1912.12115*, 2019.

[11] Y. Liu, Y. Kang, T. Zou, Y. Pu, Y. He, X. Ye, Y. Ouyang, Y.-Q. Zhang, and Q. Yang, "Vertical federated learning: Concepts, advances, and challenges," *IEEE Transactions on Knowledge and Data Engineering*, 2024.

[12] Q. Yang, Y. Liu, T. Chen, and Y. Tong, "Federated machine learning: Concept and applications," *ACM Transactions on Intelligent Systems and Technology (TIST)*, vol. 10, no. 2, pp. 1–19, 2019.

[13] G. Wang, B. Gu, Q. Zhang, X. Li, B. Wang, and C. X. Ling, "A unified solution for privacy and communication efficiency in vertical federated learning," in *Proc. of NeurIPS*, 2024.

[14] T. Qi, F. Wu, C. Wu, L. Lyu, T. Xu, H. Liao, Z. Yang, Y. Huang, and X. Xie, "Fairvfl: A fair vertical federated learning framework with contrastive adversarial learning," in *Proc. of NeurIPS*, 2022.

[15] C.-j. Huang, L. Wang, and X. Han, "Vertical federated knowledge transfer via representation distillation for healthcare collaboration networks," in *Proc. of WWW*, 2023.

[16] Y. Xing, Z. Zheng, and F. Wu, "Preventing strategic behaviors in collaborative inference for vertical federated learning," in *Proc. of KDD*, 2024.

[17] X. Jin, P.-Y. Chen, C.-Y. Hsu, C.-M. Yu, and T. Chen, "Cafe: Catastrophic data leakage in vertical federated learning," in *Proc. of NeurIPS*, 2021.

[18] L. O. Gostin, L. A. Levit, and S. J. Nass, "Beyond the hipaa privacy rule: enhancing privacy, improving health through research," 2009.

[19] Q. Zhang, B. Gu, C. Deng, S. Gu, L. Bo, J. Pei, and H. Huang, "Asysqn: Faster vertical federated learning algorithms with better computation resource utilization," in *Proc. of KDD*, 2021.

[20] B. Gu, Z. Dang, X. Li, and H. Huang, "Federated doubly stochastic kernel learning for vertically partitioned data," in *Proc. of KDD*, 2020.

[21] C. Dwork, "Differential privacy," in *International colloquium on automata, languages, and programming*, pp. 1–12, Springer, 2006.

[22] FederatedAI, "Fate: A federated learning framework." https://github.com/FederatedAI/FATE. Accessed: 2023-10-01.

[23] PaddlePaddle, "Paddlefl: A federated learning framework based on paddlepaddle." https://github.com/PaddlePaddle/PaddleFL. Accessed: 2023-10-01.

[24] M. Li, D. G. Andersen, J. W. Park, A. J. Smola, A. Ahmed, V. Josifovski, J. Long, E. J. Shekita, and B.-Y. Su, "Scaling distributed machine learning with the parameter server," in *Proc. of OSDI*, 2014.

[25] Z. Li, K. Yang, J. Tan, W.-j. Lu, H. Wu, X. Wang, Y. Yu, D. Zhao, Y. Zheng, M. Guo, *et al.*, "Nimbus: Secure and efficient two-party inference for transformers," in *Proc. of NeurIPS*, 2024.

[26] Y. Wu, N. Xing, G. Chen, T. T. A. Dinh, Z. Luo, B. C. Ooi, X. Xiao, and M. Zhang, "Falcon: A privacy-preserving and interpretable vertical federated learning system," in *Proc. of VLDB*, 2023.

[27] Y. He, X. Tan, J. Ni, L. T. Yang, and X. Deng, "Differentially private set intersection for asymmetrical id alignment," *IEEE Transactions on Information Forensics and Security*, vol. 17, pp. 3479–3494, 2022.

[28] T. J. Castiglia, A. Das, S. Wang, and S. Patterson, "Compressed-vfl: Communication-efficient learning with vertically partitioned data," in *Proc. of ICML*, 2023.

[29] Y. Li and X. Lyu, "Convergence analysis of sequential federated learning on heterogeneous data," in *Proc. of NeurIPS*, 2024.

[30] K. Bonawitz, "Towards federated learning at scale: Syste m design," in *Proc. of MLSys*, 2019.

[31] T. Castiglia, S. Wang, and S. Patterson, "Flexible vertical federated learning with heterogeneous parties," *IEEE Transactions on Neural Networks and Learning Systems*, 2023.

[32] K. Zhang, G. Wang, H. Li, Y. Wang, H. Chen, and B. Gu, "Asynchronous vertical federated learning for kernelized auc maximization," in *Proc. of KDD*, 2024.

[33] T. Chen, X. Jin, Y. Sun, and W. Yin, "Vafl: a method of vertical asynchronous federated learning," *arXiv preprint arXiv:2007.06081*, 2020.

[34] Q. Zhang, B. Gu, C. Deng, and H. Huang, "Secure bilevel asynchronous vertical federated learning with backward updating," in *Proc. of AAAI*, 2021.

[35] J. Liu, H. Xu, L. Wang, Y. Xu, C. Qian, J. Huang, and H. Huang, "Adaptive asynchronous federated learning in resource-constrained edge computing," *IEEE Transactions on Mobile Computing*, vol. 22, no. 2, pp. 674–690, 2021.

[36] A. Koloskova, S. U. Stich, and M. Jaggi, "Sharper convergence guarantees for asynchronous sgd for distributed and federated learning," in *Proc. of NeurIPS*, 2022.

[37] T. Zhang, L. Gao, S. Lee, M. Zhang, and S. Avestimehr, "Timelyfl: Heterogeneity-aware asynchronous federated learning with adaptive partial training," in *Proc. of CVPR*, 2023.

[38] H. Chen, K. Laine, and P. Rindal, "Fast private set intersection from homomorphic encryption," in *Proc. of CCS*, 2017.

[39] M. Srivatsa, L. Liu, and A. Iyengar, "Eventguard: A system architecture for securing publish-subscribe networks," *ACM Transactions on Computer Systems (TOCS)*, vol. 29, no. 4, pp. 1–40, 2011.

[40] Q. P. Herr and P. Bunyk, "Implementation and application of first-in first-out buffers," *IEEE transactions on applied superconductivity*, vol. 13, no. 2, pp. 563–566, 2003.

[41] S. Ye, L. Zeng, X. Chu, G. Xing, and X. Chen, "Asteroid: Resource-efficient hybrid pipeline parallelism for collaborative dnn training on heterogeneous edge devices," in *Proc. of MobiCom*, 2024.

[42] L. Zheng, Z. Li, H. Zhang, Y. Zhuang, Z. Chen, Y. Huang, Y. Wang, Y. Xu, D. Zhuo, E. P. Xing, *et al.*, "Alpa: Automating inter-and {Intra-Operator} parallelism for distributed deep learning," in *Proc. of OSDI*, 2022.

[43] L. All, "Appliances energy prediction." https://www.kaggle.com/loveall/appliances-energy-prediction, 2017.

[44] I. University of California, "Blogfeedback data set." http://archive.ics.uci.edu/ml/datasets/BlogFeedback, 2014.

[45] I. University of California, "Bank marketing data set." http://archive.ics.uci.edu/ml/datasets/Bank+Marketing, 2012.

[46] U. M. L. Repository, "Default of credit card clients dataset." https://www.kaggle.com/uciml/default-of-credit-card-clients-dataset, 2016.

[47] F. Pedregosa *et al.*, "Scikit-learn: Machine learning in python." https://scikit-learn.org/stable/, 2011.

[48] K. He, X. Zhang, S. Ren, and J. Sun, "Deep residual learning for image recognition," in *Proc. of CVPR*, 2016.

[49] C. Song and A. Raghunathan, "Information leakage in embedding models," in *Proc. of CCS*, 2020.

[50] K. Cheng, T. Fan, Y. Jin, Y. Liu, T. Chen, D. Papadopoulos, and Q. Yang, "Secureboost: A lossless federated learning framework," *IEEE intelligent systems*, vol. 36, no. 6, pp. 87–98, 2021.

[51] P. T. Eugster, P. A. Felber, R. Guerraoui, and A.-M. Kermarrec, "The many faces of publish/subscribe," *ACM computing surveys (CSUR)*, vol. 35, no. 2, pp. 114–131, 2003.

[52] G. Cugola and H.-A. Jacobsen, "Using publish/subscribe middleware for mobile systems," *ACM SIGMOBILE Mobile Computing and Communications Review*, vol. 6, no. 4, pp. 25–33, 2002.

[53] F. Zhao, Z. Li, X. Ren, B. Ding, S. Yang, and Y. Li, "Vertimrf: Differentially private vertical federated data synthesis," in *Proc. of KDD*, 2024.

[54] M. Abadi, A. Chu, I. Goodfellow, H. B. McMahan, I. Mironov, K. Talwar, and L. Zhang, "Deep learning with differential privacy," in *Proc. of CCS*, 2016.

[55] C. Qu, W. Kong, L. Yang, M. Zhang, M. Bendersky, and M. Najork, "Natural language understanding with privacy-preserving bert," in *Proc. of CIKM*, 2021.

NeurIPS Paper Checklist

The checklist is designed to encourage best practices for responsible machine learning research, addressing issues of reproducibility, transparency, research ethics, and societal impact. Do not remove the checklist: **The papers not including the checklist will be desk rejected.** The checklist should follow the references and follow the (optional) supplemental material. The checklist does NOT count towards the page limit.

Please read the checklist guidelines carefully for information on how to answer these questions. For each question in the checklist:

- You should answer [Yes] , [No] , or [NA] .
- [NA] means either that the question is Not Applicable for that particular paper or the relevant information is Not Available.
- Please provide a short (1–2 sentence) justification right after your answer (even for NA).

The checklist answers are an integral part of your paper submission. They are visible to the reviewers, area chairs, senior area chairs, and ethics reviewers. You will be asked to also include it (after eventual revisions) with the final version of your paper, and its final version will be published with the paper.

The reviewers of your paper will be asked to use the checklist as one of the factors in their evaluation. While "[Yes] " is generally preferable to "[No] ", it is perfectly acceptable to answer "[No] " provided a proper justification is given (e.g., "error bars are not reported because it would be too computationally expensive" or "we were unable to find the license for the dataset we used"). In general, answering "[No] " or "[NA] " is not grounds for rejection. While the questions are phrased in a binary way, we acknowledge that the true answer is often more nuanced, so please just use your best judgment and write a justification to elaborate. All supporting evidence can appear either in the main paper or the supplemental material, provided in appendix. If you answer [Yes] to a question, in the justification please point to the section(s) where related material for the question can be found.

IMPORTANT, please:

- **Delete this instruction block, but keep the section heading "NeurIPS Paper Checklist"**,
- **Keep the checklist subsection headings, questions/answers and guidelines below.**
- **Do not modify the questions and only use the provided macros for your answers**.

1. **Claims**

   Question: Do the main claims made in the abstract and introduction accurately reflect the paper's contributions and scope?

   Answer: [Yes]

   Justification: We conducted extensive case studies to support the claims we make.

   Guidelines:

   - The answer NA means that the abstract and introduction do not include the claims made in the paper.
   - The abstract and/or introduction should clearly state the claims made, including the contributions made in the paper and important assumptions and limitations. A No or NA answer to this question will not be perceived well by the reviewers.
   - The claims made should match theoretical and experimental results, and reflect how much the results can be expected to generalize to other settings.
   - It is fine to include aspirational goals as motivation as long as it is clear that these goals are not attained by the paper.

2. **Limitations**

   Question: Does the paper discuss the limitations of the work performed by the authors?

   Answer: [Yes]

Justification: We discuss the limitations of the proposed approach in the conclusion.

Guidelines:

- The answer NA means that the paper has no limitation while the answer No means that the paper has limitations, but those are not discussed in the paper.
- The authors are encouraged to create a separate "Limitations" section in their paper.
- The paper should point out any strong assumptions and how robust the results are to violations of these assumptions (e.g., independence assumptions, noiseless settings, model well-specification, asymptotic approximations only holding locally). The authors should reflect on how these assumptions might be violated in practice and what the implications would be.
- The authors should reflect on the scope of the claims made, e.g., if the approach was only tested on a few datasets or with a few runs. In general, empirical results often depend on implicit assumptions, which should be articulated.
- The authors should reflect on the factors that influence the performance of the approach. For example, a facial recognition algorithm may perform poorly when image resolution is low or images are taken in low lighting. Or a speech-to-text system might not be used reliably to provide closed captions for online lectures because it fails to handle technical jargon.
- The authors should discuss the computational efficiency of the proposed algorithms and how they scale with dataset size.
- If applicable, the authors should discuss possible limitations of their approach to address problems of privacy and fairness.
- While the authors might fear that complete honesty about limitations might be used by reviewers as grounds for rejection, a worse outcome might be that reviewers discover limitations that aren't acknowledged in the paper. The authors should use their best judgment and recognize that individual actions in favor of transparency play an important role in developing norms that preserve the integrity of the community. Reviewers will be specifically instructed to not penalize honesty concerning limitations.

3. **Theory assumptions and proofs**

   Question: For each theoretical result, does the paper provide the full set of assumptions and a complete (and correct) proof?

   Answer: [Yes]

   Justification: This paper provides a convergence proof in the appendix.

   Guidelines:

   - The answer NA means that the paper does not include theoretical results.
   - All the theorems, formulas, and proofs in the paper should be numbered and cross-referenced.
   - All assumptions should be clearly stated or referenced in the statement of any theorems.
   - The proofs can either appear in the main paper or the supplemental material, but if they appear in the supplemental material, the authors are encouraged to provide a short proof sketch to provide intuition.
   - Inversely, any informal proof provided in the core of the paper should be complemented by formal proofs provided in appendix or supplemental material.
   - Theorems and Lemmas that the proof relies upon should be properly referenced.

4. **Experimental result reproducibility**

   Question: Does the paper fully disclose all the information needed to reproduce the main experimental results of the paper to the extent that it affects the main claims and/or conclusions of the paper (regardless of whether the code and data are provided or not)?

   Answer: [Yes]

   Justification: We provide the complete code and data in the Supplementary Materials.

   Guidelines:

   - The answer NA means that the paper does not include experiments.

- If the paper includes experiments, a No answer to this question will not be perceived well by the reviewers: Making the paper reproducible is important, regardless of whether the code and data are provided or not.
- If the contribution is a dataset and/or model, the authors should describe the steps taken to make their results reproducible or verifiable.
- Depending on the contribution, reproducibility can be accomplished in various ways. For example, if the contribution is a novel architecture, describing the architecture fully might suffice, or if the contribution is a specific model and empirical evaluation, it may be necessary to either make it possible for others to replicate the model with the same dataset, or provide access to the model. In general. releasing code and data is often one good way to accomplish this, but reproducibility can also be provided via detailed instructions for how to replicate the results, access to a hosted model (e.g., in the case of a large language model), releasing of a model checkpoint, or other means that are appropriate to the research performed.
- While NeurIPS does not require releasing code, the conference does require all submissions to provide some reasonable avenue for reproducibility, which may depend on the nature of the contribution. For example
  (a) If the contribution is primarily a new algorithm, the paper should make it clear how to reproduce that algorithm.
  (b) If the contribution is primarily a new model architecture, the paper should describe the architecture clearly and fully.
  (c) If the contribution is a new model (e.g., a large language model), then there should either be a way to access this model for reproducing the results or a way to reproduce the model (e.g., with an open-source dataset or instructions for how to construct the dataset).
  (d) We recognize that reproducibility may be tricky in some cases, in which case authors are welcome to describe the particular way they provide for reproducibility. In the case of closed-source models, it may be that access to the model is limited in some way (e.g., to registered users), but it should be possible for other researchers to have some path to reproducing or verifying the results.

5. **Open access to data and code**

Question: Does the paper provide open access to the data and code, with sufficient instructions to faithfully reproduce the main experimental results, as described in supplemental material?

Answer: [Yes]

Justification: We provide the complete code and data in the Supplementary Materials.

Guidelines:

- The answer NA means that paper does not include experiments requiring code.
- Please see the NeurIPS code and data submission guidelines (https://nips.cc/public/guides/CodeSubmissionPolicy) for more details.
- While we encourage the release of code and data, we understand that this might not be possible, so "No" is an acceptable answer. Papers cannot be rejected simply for not including code, unless this is central to the contribution (e.g., for a new open-source benchmark).
- The instructions should contain the exact command and environment needed to run to reproduce the results. See the NeurIPS code and data submission guidelines (https://nips.cc/public/guides/CodeSubmissionPolicy) for more details.
- The authors should provide instructions on data access and preparation, including how to access the raw data, preprocessed data, intermediate data, and generated data, etc.
- The authors should provide scripts to reproduce all experimental results for the new proposed method and baselines. If only a subset of experiments are reproducible, they should state which ones are omitted from the script and why.
- At submission time, to preserve anonymity, the authors should release anonymized versions (if applicable).

- Providing as much information as possible in supplemental material (appended to the paper) is recommended, but including URLs to data and code is permitted.

6. **Experimental setting/details**

   Question: Does the paper specify all the training and test details (e.g., data splits, hyper-parameters, how they were chosen, type of optimizer, etc.) necessary to understand the results?

   Answer: [Yes]

   Justification: We introduce the environment and settings required for the experiments in detail in the Experiments section.

   Guidelines:

   - The answer NA means that the paper does not include experiments.
   - The experimental setting should be presented in the core of the paper to a level of detail that is necessary to appreciate the results and make sense of them.
   - The full details can be provided either with the code, in appendix, or as supplemental material.

7. **Experiment statistical significance**

   Question: Does the paper report error bars suitably and correctly defined or other appropriate information about the statistical significance of the experiments?

   Answer: [Yes]

   Justification: We present detailed numerical analysis and discussion in the Experimental Section.

   Guidelines:

   - The answer NA means that the paper does not include experiments.
   - The authors should answer "Yes" if the results are accompanied by error bars, confidence intervals, or statistical significance tests, at least for the experiments that support the main claims of the paper.
   - The factors of variability that the error bars are capturing should be clearly stated (for example, train/test split, initialization, random drawing of some parameter, or overall run with given experimental conditions).
   - The method for calculating the error bars should be explained (closed form formula, call to a library function, bootstrap, etc.)
   - The assumptions made should be given (e.g., Normally distributed errors).
   - It should be clear whether the error bar is the standard deviation or the standard error of the mean.
   - It is OK to report 1-sigma error bars, but one should state it. The authors should preferably report a 2-sigma error bar than state that they have a 96% CI, if the hypothesis of Normality of errors is not verified.
   - For asymmetric distributions, the authors should be careful not to show in tables or figures symmetric error bars that would yield results that are out of range (e.g. negative error rates).
   - If error bars are reported in tables or plots, The authors should explain in the text how they were calculated and reference the corresponding figures or tables in the text.

8. **Experiments compute resources**

   Question: For each experiment, does the paper provide sufficient information on the computer resources (type of compute workers, memory, time of execution) needed to reproduce the experiments?

   Answer: [Yes]

   Justification: We introduce the environment and settings required for the experiments in detail in the Experiments section.

   Guidelines:

   - The answer NA means that the paper does not include experiments.

- The paper should indicate the type of compute workers CPU or GPU, internal cluster, or cloud provider, including relevant memory and storage.
- The paper should provide the amount of compute required for each of the individual experimental runs as well as estimate the total compute.
- The paper should disclose whether the full research project required more compute than the experiments reported in the paper (e.g., preliminary or failed experiments that didn't make it into the paper).

9. **Code of ethics**

   Question: Does the research conducted in the paper conform, in every respect, with the NeurIPS Code of Ethics `https://neurips.cc/public/EthicsGuidelines`?

   Answer: [Yes]

   Justification: We fully follow the NeurIPS'25 policy for manuscript submission.

   Guidelines:

   - The answer NA means that the authors have not reviewed the NeurIPS Code of Ethics.
   - If the authors answer No, they should explain the special circumstances that require a deviation from the Code of Ethics.
   - The authors should make sure to preserve anonymity (e.g., if there is a special consideration due to laws or regulations in their jurisdiction).

10. **Broader impacts**

    Question: Does the paper discuss both potential positive societal impacts and negative societal impacts of the work performed?

    Answer: [Yes]

    Justification: We provide a detailed discussion of impact in the Introduction section.

    Guidelines:

    - The answer NA means that there is no societal impact of the work performed.
    - If the authors answer NA or No, they should explain why their work has no societal impact or why the paper does not address societal impact.
    - Examples of negative societal impacts include potential malicious or unintended uses (e.g., disinformation, generating fake profiles, surveillance), fairness considerations (e.g., deployment of technologies that could make decisions that unfairly impact specific groups), privacy considerations, and security considerations.
    - The conference expects that many papers will be foundational research and not tied to particular applications, let alone deployments. However, if there is a direct path to any negative applications, the authors should point it out. For example, it is legitimate to point out that an improvement in the quality of generative models could be used to generate deepfakes for disinformation. On the other hand, it is not needed to point out that a generic algorithm for optimizing neural networks could enable people to train models that generate Deepfakes faster.
    - The authors should consider possible harms that could arise when the technology is being used as intended and functioning correctly, harms that could arise when the technology is being used as intended but gives incorrect results, and harms following from (intentional or unintentional) misuse of the technology.
    - If there are negative societal impacts, the authors could also discuss possible mitigation strategies (e.g., gated release of models, providing defenses in addition to attacks, mechanisms for monitoring misuse, mechanisms to monitor how a system learns from feedback over time, improving the efficiency and accessibility of ML).

11. **Safeguards**

    Question: Does the paper describe safeguards that have been put in place for responsible release of data or models that have a high risk for misuse (e.g., pretrained language models, image generators, or scraped datasets)?

    Answer: [Yes]

Justification: We have carefully checked the published models and data and confirmed that they do not pose any risks.

Guidelines:

- The answer NA means that the paper poses no such risks.
- Released models that have a high risk for misuse or dual-use should be released with necessary safeguards to allow for controlled use of the model, for example by requiring that users adhere to usage guidelines or restrictions to access the model or implementing safety filters.
- Datasets that have been scraped from the Internet could pose safety risks. The authors should describe how they avoided releasing unsafe images.
- We recognize that providing effective safeguards is challenging, and many papers do not require this, but we encourage authors to take this into account and make a best faith effort.

12. **Licenses for existing assets**

    Question: Are the creators or original owners of assets (e.g., code, data, models), used in the paper, properly credited and are the license and terms of use explicitly mentioned and properly respected?

    Answer: [Yes]

    Justification: We fully follow the NeurIPS'25 policy for manuscript submission.

    Guidelines:

    - The answer NA means that the paper does not use existing assets.
    - The authors should cite the original paper that produced the code package or dataset.
    - The authors should state which version of the asset is used and, if possible, include a URL.
    - The name of the license (e.g., CC-BY 4.0) should be included for each asset.
    - For scraped data from a particular source (e.g., website), the copyright and terms of service of that source should be provided.
    - If assets are released, the license, copyright information, and terms of use in the package should be provided. For popular datasets, `paperswithcode.com/datasets` has curated licenses for some datasets. Their licensing guide can help determine the license of a dataset.
    - For existing datasets that are re-packaged, both the original license and the license of the derived asset (if it has changed) should be provided.
    - If this information is not available online, the authors are encouraged to reach out to the asset's creators.

13. **New assets**

    Question: Are new assets introduced in the paper well documented and is the documentation provided alongside the assets?

    Answer: [Yes]

    Justification: The new dataset is documented in the attached material.

    Guidelines:

    - The answer NA means that the paper does not release new assets.
    - Researchers should communicate the details of the dataset/code/model as part of their submissions via structured templates. This includes details about training, license, limitations, etc.
    - The paper should discuss whether and how consent was obtained from people whose asset is used.
    - At submission time, remember to anonymize your assets (if applicable). You can either create an anonymized URL or include an anonymized zip file.

14. **Crowdsourcing and research with human subjects**

Question: For crowdsourcing experiments and research with human subjects, does the paper include the full text of instructions given to participants and screenshots, if applicable, as well as details about compensation (if any)?

Answer: [NA]

Justification: Not applicable.

Guidelines:

- The answer NA means that the paper does not involve crowdsourcing nor research with human subjects.
- Including this information in the supplemental material is fine, but if the main contribution of the paper involves human subjects, then as much detail as possible should be included in the main paper.
- According to the NeurIPS Code of Ethics, workers involved in data collection, curation, or other labor should be paid at least the minimum wage in the country of the data collector.

15. **Institutional review board (IRB) approvals or equivalent for research with human subjects**

Question: Does the paper describe potential risks incurred by study participants, whether such risks were disclosed to the subjects, and whether Institutional Review Board (IRB) approvals (or an equivalent approval/review based on the requirements of your country or institution) were obtained?

Answer: [NA]

Justification: Not applicable.

Guidelines:

- The answer NA means that the paper does not involve crowdsourcing nor research with human subjects.
- Depending on the country in which research is conducted, IRB approval (or equivalent) may be required for any human subjects research. If you obtained IRB approval, you should clearly state this in the paper.
- We recognize that the procedures for this may vary significantly between institutions and locations, and we expect authors to adhere to the NeurIPS Code of Ethics and the guidelines for their institution.
- For initial submissions, do not include any information that would break anonymity (if applicable), such as the institution conducting the review.

16. **Declaration of LLM usage**

Question: Does the paper describe the usage of LLMs if it is an important, original, or non-standard component of the core methods in this research? Note that if the LLM is used only for writing, editing, or formatting purposes and does not impact the core methodology, scientific rigorousness, or originality of the research, declaration is not required.

Answer: [Yes]

Justification: This paper uses LLM to polish the language.

Guidelines:

- The answer NA means that the core method development in this research does not involve LLMs as any important, original, or non-standard components.
- Please refer to our LLM policy (https://neurips.cc/Conferences/2025/LLM) for what should or should not be described.

A Scarecrow Solution

To optimize Eq. (4), a common approach is to implement a PS architecture within each party to achieve parallel processing. This architecture is widely adopted by industrial-level VFL frameworks like FATE [22] and PaddleFL [23]. The PS architecture in VFL typically involves each party setting up a PS and a set of workers, each running a VFL executor responsible for model training and security protocols. For a given task, the coordinator, responsible for scheduling system components, determines the parallel factor ν, which specifies the number of workers to be created. It then instructs the agents of each party to initiate the PS and workers. This setup involves both inter-party Peer-to-Peer communication among workers from different parties, as well as intra-party communication between the PS and its workers, ensuring efficient coordination and execution of the VFL task [26].

Specifically, in each iteration, the P_a's PS selects a batch and divides the instance IDs into q subsets, such as $\mathrm{ID} = \{\mathrm{ID}_1, \ldots, \mathrm{ID}_q\}$. PS then broadcasts these subsets to the P_p's PS, which distributes each subset ID_j to its workers. This ensures that during execution, the PS and workers of each party are aligned, with each group of workers processing the same instances. The workers of P_a and P_p execute forward propagation concurrently, with the workers of P_a completing the remaining forward propagation and performing backward propagation using the top model. Meanwhile, once the workers of P_p receive the corresponding gradients, they carry out backward propagation to update their local models. Afterward, each worker uploads the updated model parameters to its respective PS. Finally, the PS aggregates these updates and broadcasts the refined model parameters to its workers, completing the iteration.

Limitations. While deploying the PS architecture in VFL can significantly improve training efficiency (i.e., decrease $Cost_1$ and $Cost_2$), it still faces certain limitations. Firstly, due to disparities in computational overhead among the parties, the computation times in VFL are unbalanced. Since PS must ensure strict ID alignment, the faster worker in a pair of workers must wait for the slower one, or the training process will fail due to mismatched embeddings. Moreover, deploying a PS does not fully address the issues of resource and data heterogeneity between parties, as the PS architecture cannot facilitate resource collaboration between different parties. This limits its ability to optimize resource allocation and manage data heterogeneity effectively in VFL.

Table 5: Comparison of Different VFL Architectures

Framework	**Architecture**	**Asynchronous**	**Computational Efficiency**	**Comm. Mechanism**	**Scalability**	**Fault Tolerance**	**Implementation Complexity**	**Representative Frameworks**
Pure VFL	Centralized	No	Low	Direct Peer-to-Peer	Low	Low	Low	N/A
VFL with PS	PS	No	High	Centralized PS Communication	Medium	Medium	Medium	FATE [22], PaddleFL [23]
AVFL	Centralized	Yes	Medium	Asynchronous Peer-to-Peer	Medium	Low	High	SecureBoost [50], AsyVFL
AVFL with PS	PS	Yes	High	Asynchronous PS Communication	High	Medium	High	Falcon [26]
`PubSub-VFL`	**Pub/Sub with PS**	**Yes**	**Highest**	**Efficient Pub/Sub Channels**	**Highest**	**High**	**Medium**	**Proposed System**

B Publisher/Subscriber Architecture

Pub/Sub Architecture. The Pub/Sub model consists of three primary entities: publishers, subscribers, and a message broker (or middleware). Specifically, the Pub/Sub architecture is a design pattern that facilitates communication between different parts of a software system by decoupling message senders (publishers) from message receivers (subscribers) [51]. In this model, publishers generate messages and send them to a central message broker, specifying topics or channels. Subscribers express interest in particular topics and receive messages related to those topics through the broker, without needing to know who the publishers are. This setup allows for scalable, flexible, and asynchronous communication, as publishers and subscribers can operate independently, and additional components can be added without disrupting existing interactions [52]. We summarize the advantages of the Pub/Sub architecture as follows:

- **Decoupling of Components:** Publishers and subscribers operate independently, reducing system complexity and enhancing maintainability.
- **Scalability:** The architecture supports high-throughput message dissemination, making it suitable for large-scale distributed systems.

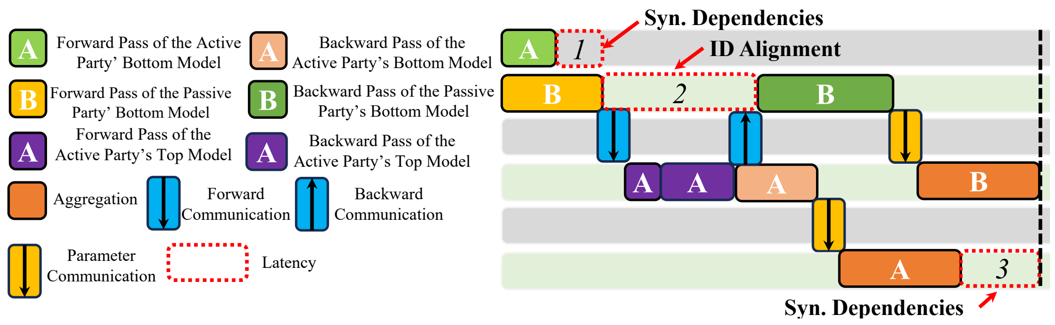
Forward Pass of the Active Party' Bottom Model
Backward Pass of the Active Party's Bottom Model
Forward Pass of the Passive Party' Bottom Model
Backward Pass of the Passive Party's Bottom Model
Forward Pass of the Active Party's Top Model
Backward Pass of the Active Party's Top Model
Aggregation
Forward Communication
Backward Communication
Parameter Communication
Latency
Syn. Dependencies
ID Alignment
Syn. Dependencies

Figure 6: Pipeline overview of the VFL with PS architecture. Synchronization dependencies may cause latency 1 and latency 3, while latency 2 is the computation dependency caused by ID alignment.

- **Fault Tolerance:** Message brokers often provide mechanisms for persistence, ensuring reliability even in the presence of failures.
- **Asynchronous Communication:** Subscribers receive messages without blocking publishers, improving system responsiveness.

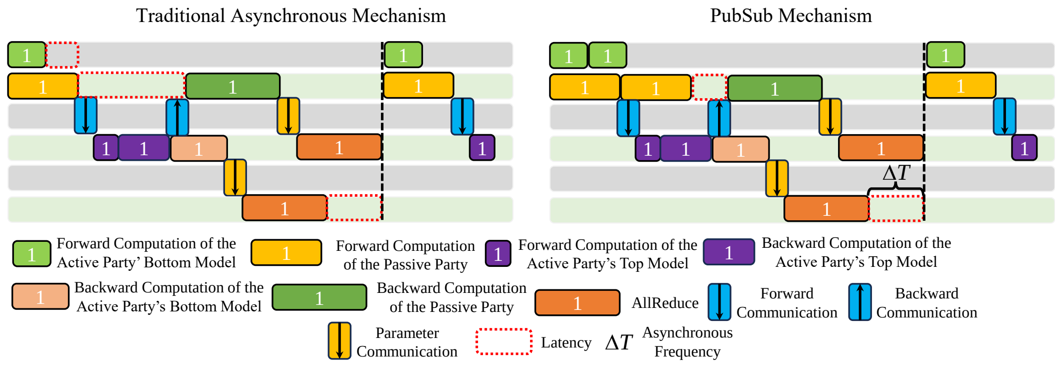
Traditional Asynchronous Mechanism
PubSub Mechanism
ΔT
Forward Computation of the Active Party' Bottom Model
Forward Computation of the Passive Party
Forward Computation of the Active Party's Top Model
Backward Computation of the Active Party's Top Model
Backward Computation of the Active Party's Bottom Model
Backward Computation of the Passive Party
AllReduce
Forward Communication
Backward Communication
Parameter Communication
Latency
ΔT Asynchronous Frequency

Figure 7: Traditional Asynchronous Mechanism *v.s.* Pub/Sub Mechanism.

Traditional Asynchronous Mechanism *v.s.* Pub/Sub Mechanism. In Fig. 7, we summarize the pipeline of the traditional asynchronous mechanism and the Pub/Sub mechanism in VFL. We found that the traditional asynchronous mechanism still has a lot of redundant latency because it is difficult to decouple from ID alignment. Because the traditional asynchronous mechanism relies on direct sender-receiver interactions using message queues, callbacks, or polling, leading to tight coupling and increased complexity as the number of workers grows. In contrast, the Pub/Sub mechanism introduces a decoupled communication model where publishers send messages to a broker, and subscribers receive relevant updates asynchronously, improving scalability and flexibility. Therefore, Pub/Sub can be well decoupled from ID alignment, so that the next task can be executed without additional waiting.

C Differential Privacy Protocol

Definition C.1 *A randomized mechanism $\mathcal{M}$ satisfies (μ, σ_{dp})-GDP if for all measurable sets S and for all adjacent datasets D and D', the following inequality holds:*

$$\mathbb{P}[\mathcal{M}(D) \in S] \leq e^{\mu}\mathbb{P}[\mathcal{M}(D') \in S] + \delta, \tag{16}$$

where μ is a privacy loss parameter, σ_{dp} is the standard deviation of the Gaussian noise added, and δ is a small probability allowing for a slight relaxation of the privacy guarantee. We explain the GDP design applicable to the embedding mechanism belows.

Unlike traditional differentially private VFL [53], which applies DP noise directly to the gradient, in SL-based VFL, privacy protection must be applied to the embedding sent by P_b to safeguard intermediate interaction results. This necessity arises because adversaries commonly exploit embedding inversion attacks [49] to infer P_b's private feature information. To ensure DP protection at the embedding level, we leverage the moments accountant technique introduced in [54] to precisely calibrate the DP noise. Specifically, we apply GDP by injecting randomized noise into selected neurons, effectively balancing privacy preservation and model utility while mitigating privacy risks in SL-based VFL. To this end, we set the variance of the Gaussian random neuron at the l-th layer as

$$\sigma_{dp} = \mathcal{O}(N_m\sqrt{K}/(\mu N)), \tag{17}$$

where N_m is the size of minibatch used at worker, N is the size of the whole batch, K is the number of queries (i.e., the number of batches processed by h at worker), then `PubSub-VFL` satisfies μ-GDP for the data of worker. This method demonstrates the trade-off between accuracy and privacy. To increase privacy, i.e., decrease μ in (16), the variance of random neurons needs to be increased (cf. (17)). However, as the variance of random neurons increases, the variance of the stochastic gradient also increases, which will in turn lead to slower convergence.

Discussion. In practice, existing VFL frameworks like FATE often employ homomorphic encryption protocols to protect the privacy of intermediate results, such as embeddings or gradients. However, these cryptographic techniques come with significant computational overhead, leading to increased costs for participants. Given that the participants in our scenarios are institutions or enterprises with a low likelihood of engaging in malicious attacks, GDP emerges as a more economical and privacy-friendly solution. Furthermore, in our experiments, we thoroughly evaluate the effectiveness of GDP in defending against various advanced inference attacks. The results demonstrate that GDP offers robust protection, making it a practical choice for preserving privacy in VFL systems without compromising performance.

D Convergence Proof

D.1 Assumptions

In this section, we provide the necessary assumptions as follows:

Assumption D.1 *(Smoothness). If the global loss function $f(\theta)$ is L-smooth, thus, we have:*

$$\|\nabla f(\theta_1) - \nabla f(\theta_2)\| \leq L\|\theta_1 - \theta_2\|, \quad \forall \theta_1, \theta_2. \tag{18}$$

Assumption D.2 *(Strong Convexity). For the purpose of this analysis, we assume that $f(\theta)$ is μ-strongly convex:*

$$f(\theta_2) \geq f(\theta_1) + \langle \nabla f(\theta_1), \theta_2 - \theta_1 \rangle + \frac{\mu}{2}\|\theta_2 - \theta_1\|^2. \tag{19}$$

Assumption D.3 *(Bounded Stochastic Gradient Variance). Let $g(\theta;\xi)$ denote the stochastic gradient computed on a mini-batch. Then we have:*

$$\mathbb{E}\left[\|g(\theta;\xi) - \nabla f(\theta)\|^2\right] \leq \sigma^2. \tag{20}$$

Assumption D.4 *(Bounded Delay/Staleness). Due to semi-asynchronous updates, the gradient used at iteration t is computed at a delayed parameter $\theta_{t-\tau(t)}$ with $\tau(t) \leq \Delta T$. We assume that the delay satisfies*

$$\|\nabla f(\theta_t) - \nabla f(\theta_{t-\tau(t)})\| \leq L \sum_{j=t-\tau(t)}^{t-1} \|\theta_{j+1} - \theta_j\|. \tag{21}$$

Assumption D.5 *(Gaussian DP Noise Injection). The Gaussian noise ξ_{dp} added to each exchanged embedding is independent with*

$$\xi_{dp} \sim \mathcal{N}(0, \sigma_{dp}^2 I), \tag{22}$$

and the variance σ_{dp}^2 is determined by the calibration formula provided. Consequently, the effective update noise is increased to

$$\sigma_{total}^2 = \sigma^2 + \sigma_{dp}^2. \tag{23}$$

Assumption D.6 *(Reliable Communication under Capacity Constraints). The Pub/Sub mechanism guarantees that embeddings (of dimension d) are delivered within the delay bound τ provided that the channel capacity p is not exceeded.*

D.2 Convergence Analysis

Based on the necessary assumptions above, we write the following convergence objective.

Theorem D.1 *If Assumptions D.1–D.6 are held and if the update rule*

$$\theta_{t+1} = \theta_t - \eta\Big(g_{t-\tau(t)} + \xi_{dp,t}\Big), \tag{24}$$

is applied with a constant learning rate η chosen sufficiently small (so that higher-order terms are negligible), there exist constants such that the expected optimality gap satisfies

$$\boxed{\mathbb{E}[f(\theta_t) - f(\theta^*)] \leq \Big(1 - 2\mu\eta + O(\eta^2 L + \eta^3 L^2 \tau)\Big)^t \Big(f(\theta_0) - f(\theta^*)\Big) + \frac{L\eta\,(\sigma^2 + \sigma_{dp}^2)}{4\mu},} \tag{25}$$

where θ^* is the unique minimizer of $f(\theta)$.

Proof D.1 *First, we review the gradient update rule. The gradient update with delay and DP noise is written as:*

$$\theta_{t+1} = \theta_t - \eta\left(g_{t-\tau(t)} + \xi_{dp,t}\right), \tag{26}$$

where $\xi_{dp,t}$ is the independent DP noise at iteration t. We then use the L-smoothness (refer to Assumption D.1), we have:

$$f(\theta_{t+1}) \leq f(\theta_t) + \langle \nabla f(\theta_t), \theta_{t+1} - \theta_t\rangle + \frac{L}{2}\|\theta_{t+1} - \theta_t\|^2. \tag{27}$$

We substitute the gradient update rule, thus, we have:

$$f(\theta_{t+1}) \leq f(\theta_t) - \eta\langle \nabla f(\theta_t), g_{t-\tau(t)} + \xi_{dp,t}\rangle + \frac{L\eta^2}{2}\|g_{t-\tau(t)} + \xi_{dp,t}\|^2. \tag{28}$$

Taking expectation conditioned on θ_t and noting that $\xi_{dp,t}$ is independent of θ_t with zero mean, we get:

$$\begin{aligned}\mathbb{E}[f(\theta_{t+1})] \leq\ & f(\theta_t) - \eta\langle \nabla f(\theta_t), \mathbb{E}[g_{t-\tau(t)}]\rangle \\ & + \frac{L\eta^2}{2}\mathbb{E}\left[\|g_{t-\tau(t)} + \xi_{dp,t}\|^2\right].\end{aligned} \tag{29}$$

Since $\mathbb{E}[g_{t-\tau(t)}] = \nabla f(\theta_{t-\tau(t)})$, and using the independence and zero mean of $\xi_{dp,t}$, thus, we have:

$$\begin{aligned}\mathbb{E}\left[\|g_{t-\tau(t)} + \xi_{dp,t}\|^2\right] =\ & \|\nabla f(\theta_{t-\tau(t)})\|^2 \\ & + \mathbb{E}\left[\|g_{t-\tau(t)} - \nabla f(\theta_{t-\tau(t)})\|^2\right] \\ & + \mathbb{E}\left[\|\xi_{dp,t}\|^2\right].\end{aligned} \tag{30}$$

By assumptions Assumptions D.3 and D.6, this yields

$$\mathbb{E}\left[\|g_{t-\tau(t)} + \xi_{dp,t}\|^2\right] \leq \|\nabla f(\theta_{t-\tau(t)})\|^2 + \sigma^2 + \sigma_{dp}^2 = \|\nabla f(\theta_{t-\tau(t)})\|^2 + \sigma_{total}^2. \tag{31}$$

Thus, the expected loss satisfies:

$$\begin{aligned}\mathbb{E}[f(\theta_{t+1})] \leq\ & f(\theta_t) - \eta\langle \nabla f(\theta_t), \nabla f(\theta_{t-\tau(t)})\rangle \\ & + \frac{L\eta^2}{2}\Big(\|\nabla f(\theta_{t-\tau(t)})\|^2 + \sigma_{total}^2\Big).\end{aligned} \tag{32}$$

Because of the delay, we need to relate $\nabla f(\theta_t)$ and $\nabla f(\theta_{t-\tau(t)})$. Under the smoothness assumption and bounded delay (refer to Assumption D.4), one can show (following standard asynchronous update arguments) that:

$$\langle \nabla f(\theta_t), \nabla f(\theta_{t-\tau(t)})\rangle \geq \|\nabla f(\theta_t)\|^2 - \delta_t, \tag{33}$$

with an error term δ_t that is on the order of $L\sum_{j=t-\tau(t)}^{t-1}\|\theta_{j+1} - \theta_j\|\,\|\nabla f(\theta_t)\|$. This error is typically bounded by a term proportional to $\eta^2 L^2 \tau\,\|\nabla f(\theta_t)\|^2$. Thus, for some constant C_1,

$$\langle \nabla f(\theta_t), \nabla f(\theta_{t-\tau(t)})\rangle \geq \|\nabla f(\theta_t)\|^2 - C_1\eta^2 L^2 \tau\,\|\nabla f(\theta_t)\|^2. \tag{34}$$

Similarly, we can upper bound $\|\nabla f(\theta_{t-\tau(t)})\|^2$ in terms of $\|\nabla f(\theta_t)\|^2$ plus a similar delay-dependent error. For simplicity in the derivation, assume that the delay-related errors yield an additional multiplicative factor of order $C_1\eta^2 L^2 \tau$.

Strong convexity (refer to Assumption D.2) implies:

$$\|\nabla f(\theta_t)\|^2 \geq 2\mu\big(f(\theta_t) - f(\theta^*)\big), \tag{35}$$

where θ^* is the unique minimizer.

Substitute the bounds back into the expected loss difference:

$$\begin{aligned}\mathbb{E}[f(\theta_{t+1})] &\leq f(\theta_t) - \eta\Big(\|\nabla f(\theta_t)\|^2 - C_1\eta^2 L^2\tau\,\|\nabla f(\theta_t)\|^2\Big)\\ &+ \frac{L\eta^2}{2}\Big(\|\nabla f(\theta_t)\|^2 + \sigma^2_{\mathit{total}}\Big)\\ &= f(\theta_t) - \eta\|\nabla f(\theta_t)\|^2\Big(1 - C_1\eta^2L^2\tau\Big)\\ &+ \frac{L\eta^2}{2}\|\nabla f(\theta_t)\|^2 + \frac{L\eta^2}{2}\sigma^2_{\mathit{total}}.\end{aligned} \tag{36}$$

Collecting the gradient terms:

$$\mathbb{E}[f(\theta_{t+1})] \leq f(\theta_t) - \eta\|\nabla f(\theta_t)\|^2\left(1 - C_1\eta^2L^2\tau - \frac{L\eta}{2}\right) + \frac{L\eta^2}{2}\sigma^2_{\mathit{total}}. \tag{37}$$

Using the strong convexity lower bound $\|\nabla f(\theta_t)\|^2 \geq 2\mu(f(\theta_t) - f(\theta^*))$, we obtain:

$$\begin{aligned}\mathbb{E}\big[f(\theta_{t+1}) - f(\theta^*)\big] &\leq \left(1 - 2\mu\eta\left(1 - C_1\eta^2L^2\tau - \frac{L\eta}{2}\right)\right)\big(f(\theta_t) - f(\theta^*)\big)\\ &+ \frac{L\eta^2}{2}\sigma^2_{\mathit{total}}.\end{aligned} \tag{38}$$

For sufficiently small η (and ignoring higher-order terms), this recursion can be written approximately as:

$$\mathbb{E}\big[f(\theta_{t+1}) - f(\theta^*)\big] \leq \big(1 - \eta\mu + C_1'\eta^2L^2\tau\big)\big(f(\theta_t) - f(\theta^*)\big) + \frac{C_2\eta^2L}{2}\sigma^2_{\mathit{total}},$$

where C_1' and C_2 are constants that incorporate the delay and smoothness effects.

Unrolling the recursion yields:

$$\mathbb{E}\big[f(\theta_t) - f(\theta^*)\big] \leq \big(1 - \eta\mu + C_1'\eta^2L^2\tau\big)^t\big(f(\theta_0) - f(\theta^*)\big) + \frac{C_2\eta L\,\sigma^2_{\mathit{total}}}{2\mu}, \tag{39}$$

or equivalently,

$$\begin{aligned}\mathbb{E}\big[f(\theta_t) - f(\theta^*)\big] &\leq \big(1 - \eta\mu + C_1'\eta^2L^2\tau\big)^t\big(f(\theta_0) - f(\theta^*)\big)\\ &+ \frac{C_2\eta L\,(\sigma^2 + \sigma^2_{dp})}{2\mu}.\end{aligned} \tag{40}$$

Here, the second term represents the error floor caused by the combined stochastic gradient noise and the additional DP noise.

Remark on DP Noise. *The additional term σ^2_{dp} in the variance $\sigma^2_{\mathit{total}}$ means that even if the algorithm converges in expectation, the asymptotic error floor is increased by the amount of DP noise injected. In practice, this is the trade-off between privacy (controlled by the noise multiplier and hence σ^2_{dp}) and accuracy (since the convergence error floor grows with σ^2_{dp}).*

E Algorithms

The pseudo code of our improved `PubSub-VFL` training process and the dynamic programming algorithm are described as follows.

Algorithm 1 `PubSub-VFL` Training Framework

```
Require: Active party $P_a$ with dataset $D_1$, Passive party $P_b$ with dataset $D_2$
Ensure: Trained models $f_a$, $f_p$, and $g$
 1: Initialize models $f_a$, $f_p$, and $g$ with random weights $\theta_1, \theta_2$
 2: Establish embedding channels $\mathcal{C}_e$ and gradient channels $\mathcal{C}_g$ with FIFO buffers
 3: Set synchronization interval $\Delta T_t$ using Eq. (5)
 4: for each global epoch $t = 1$ to $T$ do
 5:     Publisher Phase (Passive Party $P_b$):
 6:     for each worker $w_p \in P_b$ do
 7:         Sample batch $B_j$ with IDs $\{ID_1, ..., ID_B\}$
 8:         Compute embeddings $z^p = f_p(x^p; \theta_2)$
 9:         Add noise $\xi_{dp} \sim \mathcal{N}(0, \sigma_{dp}^2 I)$ to $z^p$ (GDP protocol)
10:         Publish $(z^p, B_j)$ to embedding channel $\mathcal{C}_e[B_j]$
11:     end for
12:     Subscriber Phase (Active Party $P_a$):
13:     for each worker $w_a \in P_a$ in parallel do
14:         if $\mathcal{C}_e[B_j]$ not empty then
15:             Fetch $(z^p, B_j)$ from $\mathcal{C}_e[B_j]$
16:             Compute $z^a = f_a(x^a; \theta_1)$ and $\hat{y} = g(z^a, z^p)$
17:             Calculate loss $\mathcal{L}(\hat{y}, y)$ and gradients $\nabla_{\theta_1}\mathcal{L}$, $\nabla_{z^p}\mathcal{L}$
18:             Publish $\nabla_{z^p}\mathcal{L}$ to gradient channel $\mathcal{C}_g[B_j]$
19:         else
20:             Trigger waiting deadline mechanism (skip after $T_{ddl}$)
21:         end if
22:     end for
23:     Backward Propagation:
24:     for each worker $w_p \in P_b$ do
25:         Fetch $\nabla_{z^p}\mathcal{L}$ from $\mathcal{C}_g[B_j]$
26:         Compute $\nabla_{\theta_2}\mathcal{L}$ and update $\theta_2 \leftarrow \theta_2 - \eta\nabla_{\theta_2}\mathcal{L}$
27:         Push $\theta_2$ to $P_b$'s parameter server
28:     end for
29:     Semi-Async Parameter Aggregation:
30:     if $t \mod \Delta T_t == 0$ then
31:         Aggregate $\theta_1$ from $P_a$'s workers via PS
32:         Broadcast updated $\theta_1$ to all $P_a$ workers
33:     end if
34: end for
```

F Dataset Information

We provide details of the benchmark datasets used as follows:

Energy (Appliances Energy Prediction): The Energy dataset consists of 19,735 samples with 27 features. It is used for regression tasks and focuses on predicting the energy consumption of appliances based on environmental and meteorological variables. This dataset is commonly used in energy efficiency and smart home applications.

Blog (Blog Feedback Prediction): The Blog dataset contains 60,021 samples and 280 features. It is a regression dataset designed for predicting the number of comments on blog posts based on textual and metadata features. The dataset originates from online blog platforms and is widely used in social media analytics.

Bank (Bank Marketing): The Bank dataset has 40,787 samples with 48 features. It is a classification dataset used for predicting whether a client will subscribe to a term deposit based on demographic, economic, and campaign-related features. This dataset is widely used in financial and marketing analytics.

Credit (Credit Card Default Prediction): The Credit dataset consists of 30,000 samples with 23 features. It is a classification dataset designed for predicting whether a credit card user will default on

Algorithm 2 Optimal Configuration via Dynamic Programming

```
Require: CPU cores $C_a$, $C_p$, candidate batch sizes $\mathcal{B}$, memory constraints $M_A$, $M_P$
Ensure: Optimal $(w_a^*, w_p^*, B^*)$
 1: Compute $B_{\max} \leftarrow \min\left(\left(\frac{M_A - M_{A0}}{\rho_A}\right)^{1/\chi}, \left(\frac{M_P - M_{P0}}{\rho_P}\right)^{1/\chi}\right)$
 2: Initialize DP table $dp[i][j][r] \leftarrow \infty$
 3: for each batch size $B_r \in \mathcal{B}$ where $B_r \leq B_{\max}$ do
 4:     for each $w_a \in \{P, ..., Q\}$ do
 5:         for each $w_p \in \{M, ..., N\}$ do
 6:             Calculate computation delays $T_A$, $T_P$ using Eq. (7)-(9)
 7:             Calculate communication delay $T_{comm} \leftarrow \frac{E+G}{B_b}$
 8:             Total delay $\mathcal{O}(w_a, w_p, B_r) \leftarrow \max(T_A, T_P) + T_{comm}$
 9:             if $O(w_a, w_p, B_r) < dp[w_a][w_p][B_r]$ then
10:                 Update $dp[w_a][w_p][B_r] \leftarrow O(w_a, w_p, B_r)$
11:             end if
12:         end for
13:     end for
14: end for
15: Return $(w_a^*, w_p^*, B^*) \leftarrow \arg\min dp[\cdot][\cdot][\cdot]$
```

their next payment. The dataset is sourced from financial institutions and is commonly used in risk assessment and credit scoring.

Table 6: Summary of Benchmark Datasets for PubSub-VFL Evaluation.

Dataset	Samples	Features	Task Type	Domain
Energy	19,735	27	Regression	Energy Efficiency
Blog	60,021	280	Regression	Social Media
Bank	40,787	48	Classification	Finance/Marketing
Credit	30,000	23	Classification	Finance

G Embedding Inversion Attacks

Embedding Inversion Attacks (EIA). Embedding inversion attacks aim to recover private feature representations from embeddings shared in the VFL framework. When the bottom model contains only the embedding layer, the attacker predicts the original feature by finding the nearest neighbor of each perturbed embedding in the embedding space [55]. For bottom models with additional layers, a more sophisticated optimization-based attack [49] is used. This method iteratively refines word selection vectors by minimizing the distance between the predicted feature's representations and the observed representations for each input sample. In this paper, we follow [49] to assume the adversary trains a neural network to directly map embeddings back to their original inputs. Futhermore, we assume that the adversary has access to a shadow dataset similar to the target P_b's data.

Table 7: Accuracy comparison on benchmark datasets with large model.

Dataset	Metric	VFL	VFL-PS	AVFL	AVFL-PS	Ours
Energy	**RMSE**	84.24	86.14	83.97	84.29	**83.94**
Blog	**RMSE**	23.18	23.07	22.97	23.15	**22.14**
Bank	**AUC**	94.97	94.74	95.02	95.06	**96.97**
Credit	**AUC**	83.42	85.44	84.23	82.27	**86.07**
Synthetic	**AUC**	92.74	92.67	91.54	92.21	**94.17**

H Additional Experiments

Empirical Experiments. To determine the constant $\lambda_a, \gamma_a, \lambda_p, \gamma_p, \lambda_a^{'}, \gamma_a^{'}, \varphi_a, \beta_a, \varphi_p, \beta_p, \beta_a^{'}, \varphi_a^{'}$ in the delay model, we conduct empirical experiments. Specifically, we utilize a ten-layer MLP as the bottom model and a two-layer MLP as the top model. We set $B =$

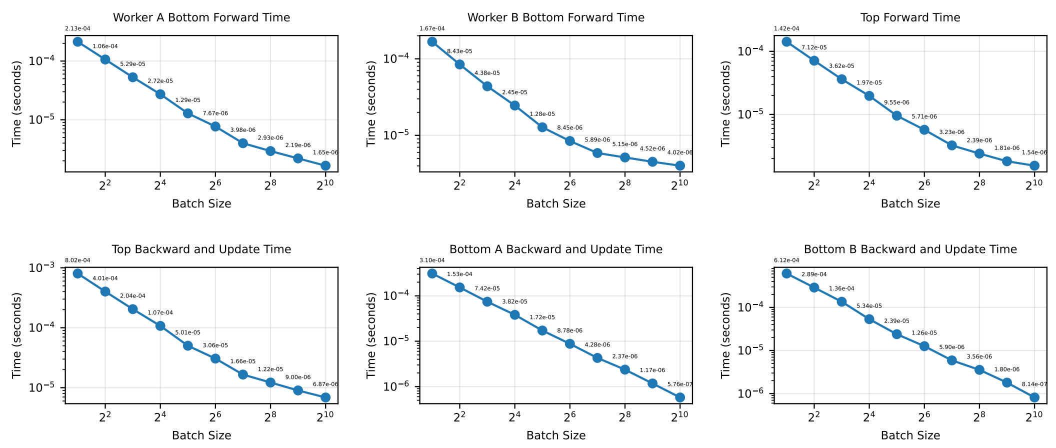

Figure 8: Empirical experimental results.

Table 8: The result of the constant being solved for.

Symbol	Value	Symbol	Value	Symbol	Value
λ_a	0.018	γ_a	-0.8015	λ_p	0.010
γ_p	-1.0071	$\lambda_a^{'}$	0.011	$\gamma_a^{'}$	-0.7514
φ_a	0.066	β_a	-0.6069	φ_p	0.038
β_p	-1.0546	$\beta_a^{'}$	-0.7834	$\varphi_a^{'}$	0.072

Table 9: Performance Comparison on Criteo 1TB Dataset.

Dataset	**Metric**	**VFL**	**VFL-PS**	**AVFL**	**AVFL-PS**	**Ours**
Criteo 1TB	AUC (%)	81.23	81.45	80.97	81.32	**82.15**
	Runtime (h)	48.6	32.1	28.9	21.5	**6.8**
	CPU Utilization (%)	42.3	65.7	58.9	72.1	**90.8**
	Waiting Time/epoch (s)	12.8	8.5	6.2	4.1	**1.3**
	Comm. Cost (GB)	1280	950	890	720	**450**

$\{2, 4, 8, 16, 32, 64, 128, 256, 512, 1024\}$ to observe the forward and backward propagation times of both participants. The experimental results are presented in Fig. 8. Based on this figure and the delay model, we derive these constants, with their computed value shown in Table 8. Note that the constants solved in different operating environments are different.

System Performance with Large Model. We compare the performance of `PubSub-VFL` and its baselines on five datasets using large models. Similar to previous evaluations, we record the best performance results and configure these methods with their optimal hyperparameters. The experimental results are summarized in Table 7. The results show that both `PubSub-VFL` and its baselines remain unaffected by the large model (i.e., ResNet), with performance showing a slight improvement. This outcome demonstrates the robustness of `PubSub-VFL` in handling large models.

System Performance on Large Dataset. To further evaluate scalability, we introduce the Criteo 1TB Click Logs dataset[3], a widely used industrial benchmark for online advertising and recommendation systems. It contains ∼4.5 billion samples with 39 features (13 numerical, 26 categorical, and high-dimensional after one-hot encoding), representing real-world big data characteristics (massive samples and sparse features). Following the evaluation metrics (AUC for classification, runtime, CPU utilization, waiting time per epoch, and communication cost) in our paper, the Table 9 below compares `PubSub-VFL` with baselines. PubSub-VFL achieves superior performance in accuracy, efficiency, resource utilization, and communication cost. It attains the highest AUC of 82.15%, outperforming baselines by 0.7–1.2%, demonstrating strong robustness in large-scale, sparse data scenarios. With hierarchical asynchrony and Pub/Sub decoupling, it reduces runtime by $\sim 3\times$ compared to AVFL-PS

[3]https://ailab.criteo.com/download-criteo-1tb-click-logs-dataset/

Table 10: Numerical results of system performance in a multi-party setting.

Method (# of Parties)	Running Time (s)	CPU Utilization (%)	Waiting Time (s)	Comm. Cost (MB)	RMSE
PubSub-VFL (10)	141.14	86.32	1.9273	896.34	23.44
PubSub-VFL (8)	121.55	88.36	2.0147	684.71	22.61
PubSub-VFL (6)	118.36	85.69	1.5697	645.34	22.34
PubSub-VFL (4)	104.72	90.14	1.2254	569.65	23.17
PubSub-VFL (2)	92.54	91.07	1.1389	439.45	22.34
VFL-PS (10)	1324.71	52.24	1.4410	1264.64	24.19
VFL-PS (8)	1374.63	47.64	1.2147	1165.17	22.61
VFL-PS (6)	1245.94	50.36	1.1647	1211.37	22.35
VFL-PS (4)	1174.65	51.24	1.4211	1089.64	23.19
VFL-PS (2)	974.65	41.47	1.2765	874.55	23.07
AVFL (10)	1445.28	27.65	20.3677	1024.34	23.54
AVFL (8)	1274.57	28.41	21.4154	967.57	23.71
AVFL (6)	1198.18	28.67	17.6517	915.16	24.01
AVFL (4)	1181.14	25.63	16.7456	847.65	22.84
AVFL (2)	1068.88	21.74	15.3657	754.77	22.97
AVFL-PS (10)	1274.51	67.51	2.6971	965.59	23.08
AVFL-PS (8)	1165.33	68.14	2.8146	817.55	23.67
AVFL-PS (6)	1017.82	58.59	2.6511	721.38	23.61
AVFL-PS (4)	1197.53	61.23	2.5636	617.45	24.07
AVFL-PS (2)	1057.67	57.68	2.4788	565.24	23.15

(6.8h vs. 21.5h) and $\sim 7\times$ compared to VFL (6.8h vs. 48.6h). It achieves high CPU utilization of 90.8%, indicating effective load balancing in heterogeneous environments, and cuts communication cost to 450GB—approximately 40% lower than AVFL-PS—through optimized channel management and reduced stale updates.

System Performance in a Multi-party Setting. While `PubSub-VFL` is currently designed and evaluated in a two-party VFL setting, its core architectural features suggest potential for extension to multi-party scenarios. The decoupled Publisher/Subscriber mechanism inherently supports many-to-many communication patterns, which is advantageous for scaling. Similarly, the hierarchical asynchronous design and buffering strategies can generalize to handle diverse update timings from multiple parties. However, the core challenges are the complexity of ID alignment and the adaptation of optimization algorithms. To address these two challenges, we provide the following two insights:

- **Complexity of ID Alignment.** To address this challenge, we can leverage existing multi-party PSI techniques (e.g., [36]), which can be applied during the system configuration phase.
- **Adaptation of Optimization Algorithms.** Because multiple parties are involved, the Dynamic Programming algorithm's search space becomes large, making it difficult to find the optimal solution. To address this challenge, a straightforward approach is to jointly model the passive party with the least resources (known from system profile information) and the active party to determine the optimal hyperparameter configuration. The key insight from doing so is that the key bottleneck dragging down system efficiency is the efficiency gap between the active party and the passive party with the least resources. This idea is consistent with the original manuscript. Although this approach is not optimal, it remains an option for expansion. In this way, our framework can be straightforwardly extended to multi-party scenarios.

The reason we did not include experiments in multi-party settings in the main text is due to the focused scope of the research topic and the intended application scenarios. We believe that incorporating both settings in a single paper might dilute the clarity and focus of the core contributions. To implement these improvements, we refactored the `PubSub-VFL` implementation by modifying several core components. Specifically, we improved the cache mechanism by increasing cache capacity to support more stable training, extended the wait deadline (T_{ddl}) to 15 seconds to enhance the reliability of embedding matching, and refined the dynamic programming optimization algorithm. All other system mechanisms were kept unchanged. Furthermore, we conducted a series of comparative experiments on the Blog dataset to evaluate the performance of PubSub-VFL in multi-party scenarios. The results are summarized in the Table 10.